

Surface and tropospheric ozone over East Asia and Southeast Asia from observations: distributions, trends, and variability

Ke Li^{1,*,#}, Rong Tan^{1,#}, Wenhao Qiao^{1,#}, Taegyung Lee², Yufen Wang¹, Danyuting Zhang¹, Minglong Tang¹, Wenqing Zhao¹, Yixuan Gu¹, Shaojia Fan³, Jinqiang Zhang⁴, Xiaopu Lyu⁵, Likun Xue⁶, Jianming Xu^{7,8}, Zhiqiang Ma^{9,10}, Mohd Talib Latif¹¹, Teerachai Amnuaylojaroen¹², Junsu Gil¹³, Mee-Hye Lee¹³, Juseon Bak¹⁴, Joowan Kim¹⁵, Hong Liao¹, Yugo Kanaya¹⁶, Xiao Lu³, Tatsuya Nagashima¹⁷, Ja-Ho Koo^{2,*}

¹State Key Laboratory of Climate System Prediction and Risk Management, Joint International Research Laboratory of Climate and Environment Change, Jiangsu Key Laboratory of Atmospheric Environment Monitoring and Pollution Control, Collaborative Innovation Center of Atmospheric Environment and Equipment Technology, School of Environmental Science and Engineering, Nanjing University of Information Science and Technology, Nanjing 210044, China

²Department of Atmospheric Sciences, Yonsei University, Seoul 03722, South Korea

³School of Atmospheric Sciences, Sun Yat-sen University, Zhuhai, Guangdong, China

⁴State Key Laboratory of Atmospheric Environment and Extreme Meteorology, Institute of Atmospheric Physics, Chinese Academy of Sciences, Beijing 100029, China

⁵Department of Geography, Faculty of Social Sciences, Hong Kong Baptist University, Hong Kong, China

⁶Environment Research Institute, Shandong University, Qingdao, China

⁷Shanghai Typhoon Institute, Shanghai Meteorological Service, Shanghai 200030, China

⁸Shanghai Key Laboratory of Meteorology and Health, Shanghai Meteorological Service, Shanghai 200030, China

⁹Institute of Urban Meteorology, China Meteorological Administration, Beijing 100089, China

¹⁰Beijing Shangdianzi Regional Atmosphere Watch Station, Beijing 101507, China

¹¹Department of Earth Sciences and Environment, Faculty of Science and Technology, Universiti Kebangsaan Malaysia, Bangi, Selangor, Malaysia

¹²Atmospheric Pollution and Climate Change Research Units, School of Energy and Environment, University of Phayao, Phayao 56000, Thailand

¹³Department of Earth and Environment Sciences, Korea University, Seoul 02841, South Korea

¹⁴Institute of Environmental Studies, Pusan National University, Busan 46241, Republic of Korea

¹⁵Department of Atmospheric Sciences, Kongju National University, Kongju 32588, South Korea

¹⁶Japan Agency for Marine-Earth Science and Technology, Yokohama, Japan

¹⁷National Institute for Environmental Studies, Tsukuba 305-8506, Japan

[#]These authors contributed equally

*Correspondence to: Ke Li (keli@nuist.edu.cn) and Ja-Ho Koo (zach45@yonsei.ac.kr)

Abstract. High level of ozone throughout the troposphere is an emerging concern over East Asia and Southeast Asia. Here we analyzed available surface ozone measurements in the past two decades (2005–2021) over eight countries, and ten ozonesonde and aircraft measurements within this region. At surface, seasonal mean ozone over 2017–2021 varies from 30 nmol mol^{-1} (i.e., 30 ppb) in Southeast Asia to 75 ppb nmol mol^{-1} in summer in North China. The metric of seasonal 95th percentile ozone can identify the multiple hotspots of ozone pollution of over 85 ppb nmol mol^{-1} in Southeast Asia. The new WHO peak season ozone standard indicates that both East Asia and Southeast Asia face a widespread risk of long-term exposure. The surface ozone increase in South Korea and Southeast Asia from 2005 was leveling off or even decreased in the past decade, while ozone increase in 2000s over China has amplified after 2013. Surface ozone trends in Japan and Mongolia were flat in the past decade. In the troposphere, the available measurements show an overall increasing tendency at different altitudes from a three-decade perspective and its trend in the past decade remains unclear due to data availability. The difference in tropospheric ozone level between East Asia and Southeast Asia is likely due to the high background ozone from stratospheric intrusion over Northeast Asia. In terms of ozone controls, our results suggest that anthropogenic emissions determine the occurrence of high ozone levels but the underappreciated strong ozone climate penalty, particularly over Southeast Asia, will make ozone controls harder under a warmer climate.

1. Introduction

Tropospheric ozone has been a long-lasting threat to public health, crop yield, and climate warming (Chang et al., 2017; DeLang et al., 2021; Lyu et al., 2023). Its importance in dampening carbon sink of forests by reducing productivity is also increasingly recognized in recent years (Cheesman et al., 2024); Zhou et al., 2024). Tropospheric ozone is mainly produced from the photochemical reactions between nitrogen oxides (NO_x) and volatile organic compounds (VOCs) in the presence of sunlight, and; stratosphere-troposphere exchange (STE) can also transport ozone into the troposphere (Neu et al., 2014) and even reach up to the surface under conducive weather conditions (Chen et al. 2024). In particular, high level of tropospheric ozone over East Asia and Southeast Asia is of great concern. For example, the estimated cardiovascular premature mortality attributable to surface ozone is 277,800 (142,900–421,900) in 2019 over East Asia and Southeast Asia, accounting for ~50% of its global health burden (Sun et al., 2024). The current surface ozone exposure can reduce the annual crop yield in China, South Korea, and Japan, by ~60, 60, 20 million tonnes for wheat, rice, and maize,

respectively (Feng et al., 2022). As such, it is important to elucidate the spatiotemporal distributions of observed ozone from the surface to troposphere over East Asia and Southeast Asia.

Surface ozone concentrations have been measured by ~~the~~ nation-level ~~network~~ networks for more than one decade in many countries. In Japan, surface network since the 1970s revealed a gradual increase in ozone (Nagashima et al. 2017; Kawano et al., 2022) until the past decade where Japanese sites experienced an ozone decrease by -0.8 ± 0.5 ~~ppb~~ nmol mol⁻¹ yr⁻¹ (Wang et al., 2024). In South Korea, surface ozone has been increasing in the past two decades, leading to the maximum daily 8 h average (MDA8) ozone often exceeding 80 ~~ppb~~ nmol mol⁻¹ in summer in the Seoul metropolitan area (Kim et al., 2023; Colombi et al., 2023). In China, national surface network was established ~~from~~ in 2013 and the widespread rising surface ozone in the past decade positioned China to be one of countries with the highest ozone level worldwide (Lu et al., 2020; Li et al., 2021; Wang et al., 2024). In contrast, Hong Kong, located in China's southern coast, exhibited an overall increase in the surface ozone level by 0.35 ~~ppb~~ nmol mol⁻¹ yr⁻¹ over 1994–2018, but the trend tended to level off in recent years (Wang et al., 2019).

In Southeast Asia, surface ozone levels are much smaller than those in East Asia due to the lower anthropogenic emissions and frequent marine air inflow (Ahamad et al., 2020; Sukkhum et al., 2022; Wang et al., 2022a). The previously published analyses on long-term ozone trends in Southeast Asia are scarce, mainly focused on Malaysia and Thailand before 2016. In Malaysia, there was observed ozone increase of 0.09–0.21 ~~ppb~~ nmol mol⁻¹ yr⁻¹ over the Peninsular Malaysia during 1997–2016 but the Borneo Malaysia recorded small or insignificant ozone trends (Ahamad et al., 2020; Wang et al., 2022a). In Thailand, the observed surface ozone experienced significant increase by 0.7 to 1.2 ~~ppb~~ nmol mol⁻¹ yr⁻¹ during dry seasons over 2005–2016 (Wang et al., 2022a). In Indonesia, there was no significant ozone trend in Bukit Koto Tabang (a suburban site) over 2005–2016 (Wang et al., 2022a). In Philippines, Salvador et al. (2022) reported an increase of 0.41 ~~ppb~~ nmol mol⁻¹ yr⁻¹ in surface ozone over 2014–2020 based on air quality measurements in Butuan (an urban site), southern Philippines. Long-term ozone measurements in other Southeast Asia countries were not well documented.

Tropospheric ozone profiles and columns over East Asia and Southeast Asia have been measured by multiple platforms including ozonesonde, aircraft, and satellite. By using long-term ozonesonde measurements, previous studies have extensively explored tropospheric ozone profiles in Beijing (Zeng et al., 2023) and Hong Kong (Liao et al., 2020) of China, and in Pohang of South Korea (Bak et al., 2022). However, these ozonesonde-based analyses mainly focused on the spatiotemporal variability and source contributions of tropospheric ozone at the individual site. By using the IAGOS (In-Service Aircraft for a Global Observing System) aircraft ozone observations, Gaudel et al. (2020)

show that tropospheric ozone level increases with latitude from Malaysia/Indonesia to Northeast China/South Korea. More importantly, they reported a rapid tropospheric ozone increase in 1994–2016 over East Asia and Southeast Asia, consistent with satellite tropospheric ozone column trends (Gopikrishnan and Kuttippurath, 2024), which has been further attributed to the rising anthropogenic emissions both locally and remotely (Wang et al., 2022a; Wang et al., 2022b; Li et al., 2023). Considering that East Asia and Southeast Asia has been identified as a global hot spot with the fastest increase in observed tropospheric ozone after 1990s by the Intergovernmental Panel on Climate Change (IPCC) Sixth Assessment Report (AR6), a comprehensive assessment on tropospheric ozone over this region by using these available measurements is strongly needed.

Under the framework of the Tropospheric Ozone Assessment Report (TOAR, 2014–2019), the TOAR documents comprehensively estimate the global ozone pollution and its historical trends. The first-phase TOAR includes only limited ground observation data over East Asia and Southeast Asia countries before 2014 (Chang et al., 2017). In the context of the TOAR Phase Two (TOAR II, 2020–2024), the established East Asia Focus Working Group (EAWG) aims to advance ozone research over East Asia and Southeast Asia, with a focus on observed ozone trends and their attributions. Our effort is to include ozone measurements (or post-calculated ozone metrics) from surface to tropopause collected from TOAR database and individual institutions over East Asia and Southeast Asia. Please also see the accompanying paper for ozone trend attributions (Lu et al., 2024).

This paper will present the most comprehensive view of ozone distributions and evolution over East Asia and Southeast Asia across different spatiotemporal scales in the past two decades. The structure of this paper is as follows: Section 2 introduces the multiple ozone measurements and calculation of different ozone metrics; Section 3 describes the present-day surface ozone levels with different metrics and long-term surface ozone trends in the past two decades; Section 4 describes the three-dimensional present-day distribution and long-term trends in tropospheric ozone; Section 5 discusses the important implications for future ozone pollution controls; Conclusions are given in Section 6.

2. Data and methods

2.1 Surface ozone observations

The TOAR data portal archives a global comprehensive and freely accessible data collection of surface ozone observations (<https://igacproject.org/activities/TOAR/TOAR-II>), which supports TOAR's assessment report of global ozone distributions and trends from surface to the tropopause. The TOAR database keeps updated to include all recent observations since 2014. To give an up-to-date assessment

of tropospheric ozone over East Asia and Southeast Asia, here we take advantage of TOAR database to examine ozone levels in different countries within the same time frame.

In this study, we used surface ozone measurements from national networks of China (2013–2021), Japan (2005–2021), South Korea (2005–2021), Malaysia (2005–2021), and Thailand (2005–2021) that were collected from the TOAR II database or provided by our EAWG members. In addition to the national network records, individual ozone measurement in Ulaanbaatar of Mongolia, Phnom Penh of Cambodia, and Bandung of Indonesia from the Acid Deposition Monitoring Network in East Asia (EANET) was also included. To assess the long-term ozone trend in China before 2013, we also collected 11 ozone measurements from previously-published literatures with updates from our EAWG members. As shown in Table S1, it includes 1 global baseline station (Mt. Waliguan), 4 regional background stations (Akedala, Longfengshan, Xianggelila, and Lin'an), and 1 rural station (Gucheng) from Xu et al. (2020), 1 regional background station (Mt. Tai) from Sun et al. (2016), 1 regional background station (Shangdianzi) from Ma et al. (2016), 1 urban station from Gu et al. (2020), and 1 urban station (Guangzhou) and 1 suburban station (Hong Kong) from Zhang et al. (2011).

To ensure data quality, the daily and monthly means were calculated using the hourly data when it has over 75% valid data each day and month. To fully assess ozone distributions, we adopted the following ozone metrics in this study: (1) Seasonal mean ozone. Seasonal MDA8 concentrations are calculated for the four seasons (December-January-February, DJF; March-April-May, MAM; June-July-August, JJA; September-October-November, SON), respectively. (2) Ozone exceedance. National ambient ozone air quality standard varies greatly among countries in East Asia and Southeast Asia (Table S2). The threshold for MDA8 ozone ranges from $60 \mu\text{g m}^{-3}$ in Philippines to $160 \mu\text{g m}^{-3}$ in China, and for the maximum daily 1 h average (MDA1) ozone ranges from $120 \mu\text{g m}^{-3}$ in Japan to $235 \mu\text{g m}^{-3}$ in Indonesia. Under standard conditions (1013 hPa, 273 K), $1 \text{ ppb nmol mol}^{-1} = 2.14 \mu\text{g m}^{-3}$. In this study, we adopted the thresholds of $60 \text{ ppb nmol mol}^{-1}$ and $47 \text{ ppb nmol mol}^{-1}$ (WHO standard) for MDA8 ozone to determine the exceedance days. (3) Peak season ozone. In 2021, the World Health Organization (WHO) newly introduced a standard for the peak season (six-month mean) ozone limit of $60 \mu\text{g m}^{-3}$ to save more people suffering from its long-term exposure. We used this threshold to assessment the peak season ozone levels.

2.2 Tropospheric ozone observations

In this part, we suggest our results from the analysis of vertical ozone profile, mostly based on the ozonesonde measurement and some aircraft measurement. There are a number of ozonesonde measurement sites, but here, we only consider 10 sites (Table S3), which has ~~10 measurements per~~

~~year at minimum, and continues~~ at least ~~5~~10 measurement years ~~continuously~~ for ~~enabling finding~~ reliable ~~characteristics, trends~~ by considering the lesson from Chang et al. (2024). If a certain site is not satisfying with this standard, we only suggest the mean pattern of ozone vertical profile for that site in order to show all existed data as possible as we can. This approach enables us to compare with recent results produced from other ozonesonde data analyses (Gaudel et al., 2024; Stauffer et al., 2024). Data at 9 sites were obtained from the World Ozone and Ultraviolet Radiation Data Centre (WOUDC), and Southern Hemisphere ADditional OZonesondes (SHADOZ) data archive. Data at Beijing site ~~was,~~ which were utilized in the previous study (Zhang et al., 2021) ~~were~~ directly provided from ~~Zhang et al. (2021), the measurement team.~~

We also used the altitudinal ozone measurements that have been collected from the In-service Aircraft for a Global Observing System (IAGOS). While the IAGOS mission has been ~~operational~~continued since 1990s and still available, ozone data in East Asia are somewhat limited. Here we only utilized the IAGOS ozone data from 1995 to ~~2014~~2022, the period having enough number of measurements, ~~for the two defined regions such as Northeast and Southeast Asia.~~ Location of all ozonesonde sites and the IAGOS region ~~are~~will be detailed in Section 4.1, and the number of all ozonesonde and IAGOS data used in this study is shown in ~~Section 4~~Figure S1.

2.3 Ozone trend calculation

Noticeable outliers are not detected in our dataset for both surface ozone and ozonesonde and IAGOS datasets. In terms of ozone distributions, we present the present-day ozone maps averaged over 2017–2021. We required that there are at least three out of these five years of data available in the calculation. In terms of ozone trends: the time frame of 2013–2021 was adopted to represent the past decade trend; the time frame of 2005–2021 was adopted to represent the 21st Century trend and time series should begin at least in the range 2005–2010 and end in the range 2017–2021; the time frame of 1995–2021 was adopted to represent the late 20th century trend and time series should begin at least in the range 1995–1999 and end in the range 2017–2021.

Following TOAR II guideline, to determine the ozone trend, we first derived the monthly anomalies of ozone concentrations that are calculated as the difference between the individual monthly means and the monthly climatology. Then, a quantile regression method as recommended by TOAR II statistical guidance was employed to estimate the linear trend in surface ozone, and a 50th quantile regression slope was reported in consideration of the length of ozone records.

3. Present-day distribution and long-term trends in surface ozone

3.1 Distribution of present-day surface ozone over 2017–2021

3.1.1 Seasonal mean MDA8 ozone

Figure 1 shows the seasonal mean MDA8 ozone concentrations averaged over 2017–2021. In winter, seasonal mean ozone level is almost below 50 ~~ppb~~ and ~~it~~ mol mol^{-1} due to the weak photochemistry. ~~In many Chinese cities, ozone concentration~~ is even decreased to 20–30 ~~ppb in many Chinese cities.~~ ~~Then~~ mol mol^{-1} , and this is because the high NO_x emissions in urban environment (e.g., North China Plain) make ozone strongly titrated and often drop below the Northern Hemisphere background ozone (Vingarzan, 2004). High ozone values of 55–60 ~~ppb~~ mol mol^{-1} in Northern Thailand and 60–65 ~~ppb~~ mol mol^{-1} in Bangkok (Thailand) are notable. In spring, seasonal mean ozone concentrations are doubled in North China (north of 30°N) and increased by 10–20 ~~ppb~~ mol mol^{-1} from wintertime in South Korea and Japan. High ozone of over 60 ~~ppb~~ mol mol^{-1} in Thailand still holds in spring and ozone concentration is enhanced by up to 20 ~~ppb~~ mol mol^{-1} in Yunan province (China), reflecting a possible concentration from spring fire emissions over Southeast Asia (Xue et al., 2021). In summer, the highest ozone levels of over 75 ~~ppb~~ mol mol^{-1} are found in the North China and western China exhibits ozone concentrations of 60–65 ~~ppb~~ mol mol^{-1} . In Southern China, ozone level is decreased to 30–55 ~~ppb~~ mol mol^{-1} because of the active summer monsoon rainfall (Zhou et al., 2022). The hot spot of summer ozone pollution is found in Seoul (South Korea) where seasonal mean ozone is also over 75 ~~ppb~~ mol mol^{-1} , followed by 55–60 ~~ppb~~ mol mol^{-1} in Tokyo (Japan), 40–50 ~~ppb~~ mol mol^{-1} in Kuala Lumpur (Malaysia), 30–40 ~~ppb~~ mol mol^{-1} in Bangkok (Thailand). In autumn, ozone concentrations are decreased strongly from their summer levels in the north of 30°N over East Asia but are increased remarkably in the Pearl River Delta (PRD) region of China where its seasonal mean MDA8 ozone of up to 65 ~~ppb~~ mol mol^{-1} is the highest level within the East Asia and Southeast Asia.

In addition to mean ozone level, Figure 2 shows the seasonal 95th percentile ozone concentrations averaged over 2017–2021. The ozone metric is almost the fifth highest value in each season, representing the high ozone values of great concern in air quality management. Although the seasonality of the 95th percentile ozone resembles the mean ozone evolution, the occurrence of the very high 95th percentile ozone values highlights the severity of ozone pollution over East Asia and Southeast Asia. In winter, high ozone of 85–95 ~~ppb~~ mol mol^{-1} occurs over the Southern Thailand, and some cities in PRD region can suffer from ozone level over 75 ~~ppb~~ mol mol^{-1} . In spring, in East Asia the 95th percentile ozone can reach over 95 ~~ppb~~ mol mol^{-1} over Chinese major city clusters and Seoul, and in Southeast Asia ozone level of over 75 ~~ppb~~ mol mol^{-1} occurs in many stations in Thailand and Peninsular Malaysia. In summer, high levels of the 95th percentile ozone appear exclusively over East

Asia, with ozone concentrations of over 115 $\mu\text{mol mol}^{-1}$ in the North China Plain (NCP), over 105 $\mu\text{mol mol}^{-1}$ in the Yangtze River Delta (YRD), and over 95 $\mu\text{mol mol}^{-1}$ in PRD, Sichuan Basin, Seoul, and Busan. In addition, some cities (e.g., Tokyo, Osaka) in Japan also have ozone levels over 85 $\mu\text{mol mol}^{-1}$. In autumn, the high ozone levels only concentrate on PRD and YRD regions, with the 95th percentile ozone over 115 $\mu\text{mol mol}^{-1}$ in PRD and over 95 $\mu\text{mol mol}^{-1}$ in YRD, respectively. However, Borneo Malaysia and Indonesia still record the 95th percentile ozone lower than 50 nmol mol^{-1} , suggesting the important role of fresh marine air inflow.

3.1.2 Number of days of ozone exceedance

Figure 3 shows that the national ozone air quality standard varies greatly in different countries over East Asia and Southeast Asia. For example, MDA8 and MDA1 ozone thresholds in China are 160 $\mu\text{g m}^{-3}$ and 200 $\mu\text{g m}^{-3}$, respectively, which lie at the high end of the adopted standards. A lower standard of MDA8 of 140 $\mu\text{g m}^{-3}$ in Thailand and of 120 $\mu\text{g m}^{-3}$ in Vietnam, South Korea, and Singapore are adopted, while Laos, Myanmar, and Philippine adopt a standard consistent with or lower than the WHO guidance. In terms of MDA1 ~~standard~~, most of the countries adopt a threshold around 200 $\mu\text{g m}^{-3}$. As such, for the sake of health impact assessment, here we adopted the uniform threshold of 60 $\mu\text{mol mol}^{-1}$ and the WHO guideline to estimate the annual ozone exceedance.

Figure 4 shows the annual number of days with MDA8 ozone concentration greater than 60 $\mu\text{mol mol}^{-1}$ (NDGT60) and with MDA8 ozone concentration greater than 47 $\mu\text{mol mol}^{-1}$ (NDGT47), respectively. In terms of NDGT60, most of the NCP cities in China have ozone exceedance over 125 days, followed by around 100 days in YRD, PRD, and Northwest China. In South Korea, most of the stations experience 60-100 days per year with daily MDA8 ozone over 60 $\mu\text{mol mol}^{-1}$, while in Japan it is almost less than 45 days except for a few cities. In Southeast Asia, NDGT60 is almost less than 75 days, and particularly Malaysia, Cambodia, and Indonesia have NDGT60 less than 15 days that is consistent with the very low 95th percentile ozone (Figure 2). If the WHO standard is applied, most of the cities in eastern China will have more than 150 days with MDA8 ozone exceedance, and this is also the case for western China. This suggests the pressing challenge to mitigate ozone pollution due to the large-scale high emissions in China. In South Korea, the NDGT47 is over 100 days for most of the stations, which is consistent with the high background ozone issue as reported by Columbi et al. (2023). Ozone exceedance over 100 days for NDGT47 can be also found in major cities in Japan, Thailand, and Malaysia.

3.1.3 Peak season ozone levels

In this study, we ~~also~~ apply the new WHO standard for peak season ozone that was introduced in

September 2021 to assess risks of long-term ozone exposure over East Asia and Southeast Asia, which has not been examined in previous studies. Figure 5 shows the estimated peak season ozone concentrations averaged over 2017-2021 and its ratio relative to the WHO standard. In China, the NCP region holds the highest peak season ozone of over 70 $\mu\text{mol mol}^{-1}$ that is about 2.5 times the WHO threshold, followed by 65 $\mu\text{mol mol}^{-1}$ in YRD, 55 $\mu\text{mol mol}^{-1}$ in PRD, SCB, and some cities of Northwest China. More importantly, the lowest peak season ozone in China is still higher than the WHO standard, suggesting the difficulty in mitigation long-term ozone exposure over China. In South Korea, the peak season ozone is well above 55 $\mu\text{mol mol}^{-1}$ and even higher than 60 $\mu\text{mol mol}^{-1}$, again reflecting the important role of background ozone in South Korea. In Japan, the peak season is mainly within the range from 40 to 55 $\mu\text{mol mol}^{-1}$, amounting to 1.5-2 times the WHO standard. In Ulaanbaatar of Mongolia, the peak season ozone is below 20 $\mu\text{mol mol}^{-1}$. In Southeast Asia, Thailand has the highest peak season ozone of over 60 $\mu\text{mol mol}^{-1}$ around Bangkok, and high values of 55-60 $\mu\text{mol mol}^{-1}$ are also found in the northern Thailand and southern coastal Thailand. In Malaysia, the Peninsular Malaysia has peak season ozone of 30-50 $\mu\text{mol mol}^{-1}$, higher than the WHO standard. However, similar with the low seasonal mean values, the Borneo Malaysia, Cambodia, and Indonesia record peak season ozone lower than the WHO standard. Overall, the estimated peak season ozone level shows that 98% stations in East Asia and Southeast Asia are above the WHO standard, and suggests the urgent need to reduce long-term ozone exposure risks.

3.1.4 Ozone climate penalty

In addition to surface ozone distributions, the metric of ozone climate penalty is also very important for understanding ozone levels under a warming change. Figure 6 shows the observed 50th percentile regression slope between MDA8 ozone and temperature in different seasons averaged over 2017-2021. In East Asia, the locations of high ozone-temperature slope of 3-5 $\text{nmol mol}^{-1} \text{ }^{\circ}\text{C}^{-1}$ in different seasons are consistent with the observed high level of surface ozone. The highest slope of over 5-8 $\text{nmol mol}^{-1} \text{ }^{\circ}\text{C}^{-1}$ is found over the PRD and Sichuan Basin in summer. In contrast, low ozone-temperature slope of less than 1 $\text{nmol mol}^{-1} \text{ }^{\circ}\text{C}^{-1}$ across different seasons can be also found in some sites over Japan and Tibetan Plateau of China, suggesting a minimal role of local ozone photochemical formation in these remote sites. In Southeast Asia, however, we find a widespread high ozone-temperature slope. In Thailand, the ozone-temperature slope of over 3 $\text{nmol mol}^{-1} \text{ }^{\circ}\text{C}^{-1}$ can be found throughout the year expect for summer. In Malaysia, a strong slope of 4-8 $\text{nmol mol}^{-1} \text{ }^{\circ}\text{C}^{-1}$ persists all the year around that is consistent with a ten-year analysis in Kuala Lumpur by Ashfold et al. (2024). More importantly, the observed 95th percentile regression shows a notably increased ozone-temperature slope over Southeast Asia (Figure S2), suggesting a stronger ozone climate penalty under extreme conditions. In contrast,

the IPCC AR6 only identified East Asia and India as the hotspot of ozone climate penalty (Zanis et al., 2022). Our observed-based results highlight the strongly underestimated ozone climate penalty over Southeast Asia.

Considering the meteorological features may be quite different in different latitudes, we conducted additional analysis on the relationship between ozone and other meteorological features (Figure S3-S7). The widespread positive (negative) correlation between ozone and temperature (relative humidity), reflecting the known conducive condition for ozone photochemistry. However, the synoptic patterns that are important for ozone transport varied greatly at a regional scale. For example, in Figure S6, summertime southerly winds are conducive for ozone pollution over North China by transporting ozone precursors and warmer air, but would decrease ozone over Southern China by carrying with cleaner marine inflow. As such, identifying the key synoptic pattern will be also necessary for understanding local ozone variations under climate change. It also deserves further study of cluster analysis about the ozone origin by transport or by precursors by taking advantage of this considerable ozone data records.

3.2 Surface ozone trends in the past two decades

3.2.1 2005-2021 ozone trends

Figure 67 shows the observed ozone trends in different seasons over the period of 2005-2021. Due to the availability of long-term surface measurements, we only present ozone trends over South Korea, Japan, Thailand, and Malaysia. In South Korea, increasing ozone trends with high certainty are notable across different seasons ranging from $0.48 \text{ ppb nmol mol}^{-1} \text{ yr}^{-1}$ in winter to $0.96 \text{ ppb nmol mol}^{-1} \text{ yr}^{-1}$ in summer. In Japan, observed ozone shows a decreasing tendency from 2005 to 2021 in summer but an extensive ozone increase by $0.28 \text{ ppb nmol mol}^{-1} \text{ yr}^{-1}$ in wintertime. In Thailand, there is an overall increasing trend in surface ozone but with spatial heterogeneity over 2005-2021. Specifically, significant ozone increase mainly occurs over northern Thailand and southern coastal Thailand, while ozone increase around Bangkok is much smaller or insignificant. In Malaysia, there is a wintertime ozone increase by $0.2 \text{ ppb nmol mol}^{-1} \text{ yr}^{-1}$ particularly in three sites in Peninsular Malaysia and in five sites in Borneo Malaysia, while in other seasons the observed ozone trends over 2005-2021 are small and statistically insignificant. The estimated increasing tendency in surface ozone since 2005 is in agreement with Kim et al (2023) for 2001-2021 ozone increase in South Korea and with Wang et al. (2022) for 2005-2016 ozone increase in Southeast Asia.

Due to the lack of national network measurement before 2013 in China, we also compiled 11 individual

ozone measurements (8 background/rural sites and 3 urban sites) that are available from around 2005 (see Data and methods). Figure 78 and Table S1 show the estimated seasonal ozone trends in these 11 stations by using the metrics of MDA8 ozone and 24-hour mean ozone. The Mt. Waliguan, a global baseline station of the World Meteorological Organization /Global Atmosphere Watch (Xu et al., 2020), shows statistically significant ozone increase by $0.56 \text{ ppb nmol mol}^{-1} \text{ yr}^{-1}$ in spring. However, at the multiple regional background stations located in western boundary of China (Xianggelila, Akedala) and eastern boundary of China (Lin'an, Longfengshan), there is no such a consistent ozone increase but with large variability across different seasons, suggesting the important role of regional emission change and climate variability (Zhang et al. 2023, Ye et al., 2024). In the NCP, one of the regions with the highest present-day ozone level, the observed ozone after 2005 at the regional background sites (Shangdianzi, Mt. Tai) and rural site (Gucheng) experienced a consistently increasing trend in spring and summer seasons. In Shangdianzi, the MDA8 ozone trend over 2005-2019 is $0.85 \text{ ppb nmol mol}^{-1} \text{ yr}^{-1}$ ($p < 0.1$) in spring and $0.73 \text{ ppb nmol mol}^{-1} \text{ yr}^{-1}$ ($p = 0.12$) in summer, respectively. The similar seasonal trends are also shown in Gucheng (a rural site close to Shangdianzi) and Mt. Tai (located in the center of NCP). It is noted that summer ozone trends in Mt. Tai over 2005-2019 also have strong intraseasonal variability, with much faster ozone increase in July and August (Sun et al., 2016). In addition to the background/rural sites, urban sites in YRD (Xujiahui) and PRD (Guangzhou, Hong Kong) record the urban ozone increase after 2005 that has been attributed to anthropogenic emissions and circulation patterns in previous studies (Wang et al., 2019; Gu et al., 2020; Cao et al., 2024).

3.2.2 2013-2021 ozone trends

Figure 89 shows the observed ozone trends in different seasons over the period of 2013-2021. Here we include ozone trends over China, Mongolia, Japan, South Korea, Malaysia, and Thailand. In China, there is a widespread ozone increase throughout the year, with mean ozone increase of $1.0\text{-}1.2 \text{ ppb nmol mol}^{-1} \text{ yr}^{-1}$ in different seasons, which is only half of the ozone increase over 2013-2019 in China (Lu et al., 2020; Li et al., 2020). Spatially, ozone increase mainly occurs in the northern China and western China. Seasonally, there is fast ozone increase in winter over the NCP region, suggesting the urgency of wintertime ozone regulation (Li et al., 2021). In South Korea, the 2005-2021 ozone rise is strongly mitigated over 2013-2021 when summer ozone trend is only $0.45 \text{ ppb nmol mol}^{-1} \text{ yr}^{-1}$. In Mongolia, there is a notable spring ozone increase but with low certainty. In Southeast Asia, however, the observed ozone in Malaysia and Thailand shows a decreasing tendency in most of the sites, which is contrary to the ~~overall~~ ozone increase from 2005 to 2021. Overall, except for the rapid ozone increase over China in the past decade, there is a leveling off or decrease in surface ozone trend over other countries in the meantime.

To further examine the long-term ozone variability, we also show the time series of observed national MDA8 ozone concentrations during warm seasons from 2005 to 2021 in Figure 910. In South Korea, there is a flat trend in ozone over 2017-2021 after a sustained ozone increase since 20152005, and there is no clear trend in warm-season ozone in Japan due to the limited data availability. In Southeast Asia, after 2013, surface ozone in Malaysia starts to decline and ozone trend in Thailand levels off. This is also demonstrated in the warm-season ozone trend in Figure S1S8. In addition, we also find the large interannual variability in observed ozone concentration that deserves further investigation. For example, in 2017, there is strong surface ozone enhancement relative to 2016 in China, Japan, and South Korea, while surface ozone is consistently decreased in Mongolia, Thailand, and Malaysia. Previous studies have linked the changes in large-scale circulations to this extensive ozone anomalies (e.g., Yin et al., 2010; Jiang et al., 2021).

4. Present-day distribution and long-term trends in tropospheric ozone profiles

4.1 Three-dimensional distribution of present-day tropospheric ozone

First, we compared climatological mean vertical ozone profile (from surface to 10 km altitude) using the ozonesonde data (Figure 1011). Beijing site in China shows the highest, but Sepang-JayaKuala Lumpur site in Malaysia shows the lowest ozone mixing-ratiomean values through the troposphere. In general, ozone mixing-ratiovalues in East Asia (Beijing in China, Pohang in Korea, and Tsukuba in Japan) isare higher than thathose in Southeast Asia (Sapang-JayaKuala Lumpur in Malaysia and Watukosek in Indonesia). This pattern is wellalso found when we compared average ozone mixing ratiovalues at 1, 3, 5, and 7 km altitudealtitudes (Figure 1112). While some sites show the higher ozone mixing-ratiovalues in the boundary layer (e.g., Watukosek), but generally free tropospheric (above 1-2 km height) ozone mixing-ratio-isvalues are higher. Especially, Beijing, Pohang, Sapporo, and Tsukuba sites show large enhancement of ozone above 8 km altitude (Figure 11a12a), implying that the stratospheric ozone is used-to-be-strongly intrudedintruding into the troposphere. Actually ozone mixing-ratio values in these 4 sites are highest at 3, 5, and 7 km altitudes, indicating the effect of stratospheric ozone to the enhancement of upper tropospheric ozone. These 4 sites are located over Japan and the Korean peninsula (Figure 1011) where sudden increase of ozone usually occurs below the tropopause (Park et al., 2012).

Seasonal pattern of vertical ozone profile was continually investigated (Figure 1213). Tropospheric

ozone values at Beijing, Pohang, Sapporo, and Tsukuba ~~sites~~ where strong stratospheric ozone intrusion occurs, are generally high in spring (MAM) and summer (JJA). This pattern can be explained by the frequent intrusion of stratospheric ozone in spring (Park et al., 2012), and strong photochemical ozone production that is typical characteristic in summer. In several sites (e.g., Beijing and Tsukuba), photochemical ozone production in summer makes the boundary layer ozone much higher than free-tropospheric ozone. Stratospheric ozone intrusion in these 4 sites ~~is~~ looks also strong in winter, but does not result in high ~~tropospheric~~ ozone in the boundary layer due to weak photochemistry in winter. ~~Ozone~~ Boundary layer ozone values at Kagoshima (Japan), Naha (Japan), King's park (Hongkong), and Hanoi (Vietnam) that are located below 30 °N, however, are lowest in ~~the lower troposphere~~ summer. Considering that these sites are easily affected by the inflow of maritime air mass under the trade-wind influence, this low summertime ozone can be explained by the transport of humid and ozone-poor air mass from the ocean due to the monsoon system (Zhao and Wang, 2018; Jiang et al., 2021). Sites in equatorial region (i.e., Sepang JayaKuala Lumpur and Watukosek) do not have large seasonal ~~variation~~ difference of tropospheric ozone.

We repeated same analysis using the IAGOS data (Figure ~~13~~ 14). IAGOS ozone profiles over Northeast Asia also reveal the highest tropospheric ozone in summer (June), and lowest in winter (December). We can also see large enhancement of summertime ozone in the boundary layer associated with strong photochemistry, and ~~highest~~ high ozone in winter (DJF) and spring (MAM) above 8 km altitude, implying the intrusion effect of stratospheric ozone. Monthly variation of ozone at multiple heights (Figure 13b) illustrates a sharp drop of ozone from June to July, depicting the wash-out effect due to the rainy season called Jangma (Korea) or Maiyu (China). Overall, ozone profile pattern in Northeast Asia from the long-term aircraft monitoring is similar to findings based on ozonesonde measurements. Among them, we would highlight that the site showing high tropospheric ozone (e.g., Beijing in China, Pohang in Korea, Sapporo in Japan), which are located in Northeast Asia and latitude is higher than 35 °N (Table S3), relate to the strong intrusion of stratospheric ozone. Considering recent studies addressing that background ozone in Northeast Asia is unexpectedly high (Lee and Park, 2022; Columbi et al., 2023), we need to put more weight on the study about the contribution of stratospheric air masses to the Northeast Asian background ozone. ~~Also~~

We also added analyzed results using the IAGOS measurements in Southeast Asia (Figure 14). It is

similar that ozone in spring (MAM) is the highest. However, ozone in winter (DJF) is not the lowest but ozone in summer (JJA) is the lowest in Southeast Asia, probably due to the relatively stronger precipitation in summer, and warmer temperature in winter, compared to the atmospheric condition in Northeast Asia. Similar to the case in Northeast Asia mentioned above, some previous studies reported cases of the tropospheric ozone enhancement in Southern China affected by the influence of typhoon (Zhan and Xie, 2022; Li, F. et al., 2023), which are typically explained based on the stratospheric ozone intrusion driven by the deep convection (Chen et al., 2022). While those reported cases look significant, however, our results in sites typically affected by typhoon (e.g., Naha, King's park) reveal that it may not contribute to significant increase of summertime mean tropospheric ozone. ~~We also added analyzed results using the IAGOS measurements in Southeast Asia, but the measurements were performed in some limited periods. There is no available data after 2012, and the number of data is enough to analyze only for the year 1995, 1996, 1997, 1999, and 2005. Thus, we did not deeply interpret IAGOS results in Southeast Asia, but simply reported themselves.~~

As stated in chapter 2.2, there are additional ozonesonde sites in East Asia, but these sites do not have long-term measurements. While we cannot provide the long-term trend values for these sites, at least the seasonal mean pattern can be suggested in spite of their short history of measurements. In this purpose, we added one more result showing the seasonal mean pattern of ozone vertical profile at additional 6 sites not having ozonesonde measurements in continuous 10 years (Figure S9): 5 sites in South Korea (Yongin, Osan, Seosan, Anmyeon, and Cheju) and 1 site in Taiwan (Taipei) obtained from the experiment team (Kang et al., 2024) or from the WOUDC data archive. Owing to the short-term property, we cannot generalize this result as the typical seasonal average. However, it seems that this information will be a good reference when the vertical ozone distribution is needed in further studies about the East Asian tropospheric ozone.

4.2. Altitudinal long-term trends of tropospheric ozone

In addition to the spatial distribution of tropospheric ozone, we ~~investigate~~investigated the long-term trend of ozone ~~mixing-ratio~~values in a vertical scale using the ozonesonde measurements. We confirmed the time-series analysis at each altitude (Figure ~~S2S10~~) and performed the ~~Mann-Kendall test~~quantile regression. Finally, we estimated long-term ozone trend in the troposphere (from surface to 10 km altitude) per 100 m interval vertically with the certainty information ~~of statistical~~

significance (using median and p-value). These results are shown in Figure 1415.

At first, we can see increasing trend of tropospheric ozone in some in most East Asian sites that we are treating examined based on the annual median value. Increasing trends of ozone mixing ratio about 1–2% per year is found values at Sapporo, Naha Tsukuba, and Hanoi consistently Naha look high certain through whole troposphere (Figure 14a, 14e Figures 15a, 15b, and 14g). Tsukuba 15e), and those at Pohang sites have similar pattern also looks partially high certain. Ozone at Hanoi mostly shows increasing trends but smaller trend (~0.5–1 % per year) having low certainty. Ozone values in King's park, Sepang Jaya Kuala Lumpur, and Watukosek are only increasing in the boundary layer (below ~2–3 km), but reveal almost no significant evident long-term trend in the free troposphere. Kagoshima and Beijing sites are totally opposite; There are decreasing trends through whole troposphere. Ozone decrease at Kagoshima mostly looks to have low certainty, but that at Beijing does not look clearly evident. In brief, we can classify 3 types of long-term trends of tropospheric ozone in East Asia: (1) Increase through whole troposphere, (2) Increase only in the boundary layer and no clear evident trend in the free troposphere, and (3) Decrease through whole troposphere.

We also examined trends using the seasonal mean ozone mixing ratio: values: spring (MAM) in Figure S3, S11, summer (JJA) in Figure S4, S12, autumn (SON) in Figure S5 S13, and winter (DJF) in Figure S6. Overall, we can split two different patterns such as seasonally consistent and inconsistent trends. Tropospheric ozone S14. Ozone increase at Sapporo, Tsukuba, and Naha has been consistently, regions showing increasing trends in all seasons. In contrast, Tropospheric ozone at Beijing reveals consistent decreasing trend, only of annual median ozone with some exception. Some exceptions are increasing trends near the surface in DJF and MAM. While these are not statistically significant, it seems required to put our eyes here more because near-surface ozone increase in high polluted area directly connects to the human health and crop damage. We can state that tropospheric ozone trend at King's park (increasing), Hanoi (increasing), and Kagoshima (decreasing) certainty, is rather consistent in all seasons, but the extent of trend varies largely according to the season. Trends at Pohang, Sepang Jaya, Watukosek are seasonally different. Ozone trends at Pohang are clearly positive in JJA and SON but almost none or even partly negative in upper heights in DJF and MAM Trends at Sepang Jaya are only positive in DJF, but generally none or negative also high certain in summer, but less certain in other seasons. Ozone at Watukosek shows the distinguished increasing only in MAM. These features

~~imply that a certain season has matchless trend~~trends at Pohang are seasonally different: increase in summer and autumn (Figures S12c and S13c), but decrease in the wintertime upper troposphere (Figure S14c). Ozone trends at Hanoi are generally increasing in terms of annual median value, but those almost become no evident in the seasonal analysis. Ozone values in King's park, Kuala Lumpur, and Watukosek, similar to the annual median analysis, are increasing with medium certainty in the boundary layer, particularly in spring and summer. In other seasons, however, ozone trends at Hanoi become no evident.

Ozone trends at Kagoshima and Beijing are different from other sites, as shown in the annual median analysis in Figure 15. They are also decreasing consistently in whole seasons. These decreasing trends at Kagoshima and Beijing are not usually accompanied with high certainty, but decreasing trends at Kagoshima in spring are high certain (Figure S11d). Although trend values are not largely evident, tropospheric ozone decrease at Beijing is quite consistent in all seasons. Zhang et al. (2021) also treated the variation of ozonesonde measurements at Beijing, and it looks that the stratospheric ozone intrusion is strong from 2006 to 2012 but not in other years, which may be related to the ozone trend at Beijing. At this present moment, these decreasing trends were not well explained by our knowledge. Nonetheless, we would report these trends because it ~~can lead whole trend pattern in that site~~be a motivation of further research.

We finally estimated the long-term trend of tropospheric ozone in East Asia using the IAGOS aircraft measurements ~~(Figure S7):~~ Northeast and Southeast Asia, separately, and analyses based on annual and seasonal median pattern (Figures S15 and S16). Data is ~~only~~ available from 1995 to ~~2014~~2022, therefore recent decade situation (e.g., the outbreak of Coronavirus disease 2019) ~~is not included here~~probably affects the trend result. In spite of this ~~limitation~~condition, generally we can see the increasing ~~trend~~trends of tropospheric ozone in East Asia, consistent with previous reports (Wang et al., 2019; Lee et al., 2021; Li, S. et al., 2023). ~~Seasonally, however, trends are rather different; There are clear increasing trends during JJA and SON, but almost no trend with partial decreasing trend in the upper troposphere during DJF and MAM. Partial decreasing trends in DJF and MAM look similar to a recent report addressing that stratospheric ozone transport to the troposphere in has been weakened (Chen et al., 2024), but overall, tropospheric ozone in East Asia reveals large increasing trends in warm season (JJA and SON), and it seems to lead to an overall ozone increase in East Asia. Compare to~~

trends in Northeast Asia, it seems that the increasing trend in Southeastern Asia looks more evident. In particular, ozone trends in Southeast Asia shows high certainty from the surface to ~ 8km consistently (Figure S16). In contrast to the continuous ozone increase in Northeast Asia, however, it seems that the ozone increase in Southeast Asia became weaker recently (Figure S17), requiring the necessity to put on our eye constantly in the future. Seasonal median trends are usually similar to annual trends except winter (DJF). Wintertime trends at Northeast Asia are partly negative in the upper troposphere (different from consistent increasing trends in other seasons), and not evident near the surface (different from increasing trends with high and medium certainty in other seasons). In Southeast Asia, wintertime ozone trends are still increasing, but mostly not evident, different from increasing trends with high certainty in other seasons.

5. Implications for ozone control

Our ~~research reveals~~ results reveal significant spatial and seasonal ozone variations over East Asia and Southeast Asia. Spatially, ozone levels are closely associated with anthropogenic emissions (e.g., NO_x emissions), with high ozone concentrations aligning well with the estimated NO_x emission patterns ~~observed through ground-based and satellite measurements.~~ Figure ~~15~~ 16 shows the bottom-up NO_x emissions and the satellite-derived NO₂ columns over East Asia and Southeast Asia. Seasonally, ozone variations are primarily influenced by meteorological conditions and biomass burning emissions in Southeast Asia. For example, ozone peaks usually occur in northern China during summer, in the Pearl River Delta during autumn, and in Southeast Asia during spring.

Relative to East Asia, although the health risks in Southeast Asia ~~are relatively~~ tend to be low under short-term ozone exposure ~~indicators~~ metrics (e.g., 95th percentile MDA8 ozone ~~concentration~~), ozone exceedance days are still notable if WHO standard is applied. The diverse short-term ozone air quality standards in Southeast Asian countries (Figure 3) suggest a great challenge to call for regional joint ozone control. Moreover, the WHO newly introduced peak season ozone concentration standard indicates that both East Asia and Southeast Asia are faced with a widespread risk of long-term ozone exposure, with the vast majority of the region exceeding the WHO ~~standards~~ standard. In addition to health impacts, the pervasive ozone pollution in East Asia and Southeast Asia is also threatening global food security by its accounting for over 60% of global rice yield (Feng et al. 2022; Yuan et al., 2022). For example, the year-around mean MDA8 ozone over 40 ~~ppb~~ nmol mol⁻¹ over Southeast Asia suggests the high ozone exposure over a threshold of 40 ~~ppb~~ nmol mol⁻¹ (AOT40) that is commonly used to

investigate ozone effects on vegetation yield (Feng et al. 2022).

~~In addition to the well known fast changing anthropogenic emissions over East Asia (Zheng et al., 2018) and Southeast Asia (Wang et al., 2022), our study shows that there is a very strong ozone climate penalty over East Asia and Southeast Asia. Figure 16 shows the observed 50th percentile regression slope between MDA8 ozone and temperature in different seasons averaged over 2017–2021. In East Asia, the locations of high ozone temperature slope of 3–5 ppb °C⁻¹ in different seasons are consistent with the observed high level of surface ozone. The highest slope of over 5–8 ppb °C⁻¹ is found over the PRD and Sichuan Basin in summer. In Southeast Asia, however, we find a widespread high ozone temperature slope. In Thailand, the ozone temperature slope of over 3 ppb °C⁻¹ can be found throughout the year except for summer. In Malaysia, a strong slope of 4–8 ppb °C⁻¹ persists all the year around that is consistent with a ten-year analysis in Kuala Lumpur by Ashfold et al. (2024). More importantly, the observed 95th percentile regression shows a notably increased ozone temperature slope over Southeast Asia (Figure S8), suggesting a stronger ozone climate penalty under extreme conditions. In contrast, the IPCC AR6 only identified East Asia and India as the hotspot of ozone climate penalty (Zanis et al., 2022). Our observed-based results highlight the strongly underestimated ozone climate penalty over Southeast Asia.~~

The long-term trend of surface ozone indicates that, based on the available data, high-emission regions in South Korea, Southeast Asia, and China have generally experienced an increase in ozone levels since 2005. However, since 2013, the increase in ozone levels in China has significantly accelerated, while the ozone trends in Thailand and Malaysia in Southeast Asia show no significant changes. Therefore, it is still urgent to attribute the varying ozone trends in East Asia and Southeast Asia across different seasons over the past decade.

In the troposphere, the available ozonesonde and IAGOS measurements not only demonstrate the high background ozone in warm seasons over Northeast Asia, but also show an overall increasing tendency in the past three decades. While the increase in tropospheric ozone can be largely attributed to the increased anthropogenic emissions as demonstrated in our companion paper (Lu et al., 2024), the origin of high seasonal background ozone in Northeast Asia remains unclear. Recent studies provide some observational and modeling evidence of stratospheric intrusion (Chen et al., 2024; Columbi et al., 2023) to explain this high background ozone, but a quantitative assessment is urgently needed. In particular, the recent ASIA-AQ campaign (<https://espo.nasa.gov/asia-aq>) flying across Asia countries would be important to understand the high tropospheric ozone issue over East Asia and Southeast Asia.

6. Conclusions

Under the framework of the TOAR II (2020-2024) that aims to estimate global and regional tropospheric ozone pollution and its historical trend, in this study we present the most comprehensive view of ozone distributions and evolution over East Asia and Southeast Asia across different spatiotemporal scales in the past two decades. This is done by taking advantage of the available surface ozone measurement in the past two decades (2005-2021) over eight countries, and ten ozonesonde and in-service aircraft measurements within this region. The key conclusions are as follows:

Firstly, there are significant spatial and seasonal ozone variations at the present-day level. In summer, seasonal mean MDA8 ozone averaged over 2017-2021 varies from 30 $\mu\text{mol mol}^{-1}$ in Southeast Asia to over 75 $\mu\text{mol mol}^{-1}$ in summer in North China and Seoul. Southeast Asia in winter and spring has high mean ozone of 60 $\mu\text{mol mol}^{-1}$ in Thailand. The seasonality of the 95th percentile ozone resembles the mean ozone evolution, but the widespread occurrence of the very high 95th percentile ozone of over 85 $\mu\text{mol mol}^{-1}$ highlights the severity of ozone pollution. If the WHO standard is applied for short-term exposure, a large fraction the sites will have more than 100 days with MDA8 ozone exceedance. In terms of long-term exposure, the WHO newly-introduced peak season ozone standard indicates that both East Asia and Southeast Asia are faced with a widespread risk of long-term ozone exposure.

Secondly, the surface ozone increase in the past two decades is widespread. In particular, South Korea has a national ozone increase with high certainty across different seasons. In Thailand, there is an overall increasing trend in surface ozone but with spatial heterogeneity over 2005-2021. In China, the compiled 11 individual measurements show an overall ozone increase in high-emission regions and at a global baseline station. However, the observed national surface ozone increase in South Korea and Southeast Asia from 2005 is leveling off or even decreased in the past decade (2013-2021), while ozone increase in 2000s over China has amplified after 2013. Surface ozone trends in Japan and Mongolia are generally flat in the past decade.

Thirdly, in the troposphere, the high ozone levels in spring and summer at Beijing, Pohang, Sapporo, and Tsukuba site are driven by strong photochemical ozone production and stratospheric ozone intrusion, supported by both the ozonesonde and IAGOS measurements. The difference in tropospheric ozone level between East Asia and Southeast Asia is likely due to the high background ozone from stratospheric intrusion over Northeast Asia. In terms of ozone trends, from a three-decade perspective,

the available ozonesonde and aircraft measurements show an overall increasing tendency at different altitudes but feature with strong site-by-site differences. Due to measurement availability, ozone trend in the past decade is still unquantified.

Fourthly, the significant spatial ozone variations over East Asia and Southeast Asia are closely associated with anthropogenic emissions, supported by ground-based and satellite measurements. Our study also shows that there is a very high ozone climate penalty over East Asia and Southeast Asia, and the widespread high ozone-temperature slope of 3-8 $\text{ppb nmol mol}^{-1} \text{ }^{\circ}\text{C}^{-1}$ persists all the year around in Southeast Asia. More importantly, the observed 95th percentile regression shows a notably increased ozone-temperature slope over Southeast Asia, suggesting a critical issue in future ozone controls.

Data availability. The sources for all data used in this study, including the observations, meteorological reanalysis and emission data will be provided upon the publication of the manuscript.

Supplement. The supplement related to this article is available online.

Author contributions. K.L. and J.H.K. led and organized the project, working as the co-leads of the East Asia Working Group of Tropospheric Ozone Assessment Report Phase II (TOAR II) with X.L. and T.N. S.J.F., J.Q.Z., X.P.L., L.K.X., J.M.X., Y.X.G., Z.Q.M., M.T.L., T.A., J.G., M.H.L., J.B., J.K., J.H.K., X.L., and T.N. assisted in preparation of observational data. K.L., R.T., W.H.Q., and J.H.K. conducted the analysis and prepared the figures. T.L., Y.F.W., D.Y.T.Z., M.L.T., W.Q.Z. contributed to preparing the figures. K.L. and J.H.K. led the writing of the manuscript. All authors contributed to improving the manuscript.

Competing interests. Some authors are members of the editorial board of Atmospheric Chemistry and Physics.

Acknowledgements. We greatly thank the China's Ministry of Ecology and Environment, Korean

Ministry of Environment, National Institute for Environmental Studies, Malaysia Department of Environment, Thailand Pollution Control Department, the Acid Deposition Monitoring Network in East Asia (EANET), World Ozone and Ultraviolet Radiation Data Centre (WOUDC), and In-service Aircraft for a Global Observing System (IAGOS) for running the ozone observation networks. MOZAIC/CARIBIC/IAGOS data were created with support from the European Commission, national agencies in Germany (BMBF), France (MESR), and the UK (NERC), and the IAGOS member institutions (<http://www.iagos.org/partners>). The participating airlines (Lufthansa, Air France, Austrian, China Airlines, Hawaiian Airlines, Air Canada, Iberia, Eurowings Discover, Cathay Pacific, Air Namibia, Sabena) supported IAGOS by carrying the measurement equipment free of charge since 1994. The data are available at <http://www.iagos.fr> thanks to additional support from AERIS. We also thank the previous and current TOAR Steering Committee members (Owen Cooper, Lin Zhang, and Keding Lu) for effortless support of guiding the East Asia Working Group of Tropospheric Ozone Assessment Report Phase II (TOAR II-), and the SHADOZ team (Anne M. Thompson, Ryan M. Stauffer and Debra E. Kollonige) for their remarkable contribution to the database of long-term ozone profile measurements.

Financial support. This research was supported by the National Natural Science Foundation of China (grants 42293323, 42205114, and 42293321), the Natural Science Foundation of Jiangsu Province (BK20240035). This work was also supported by the National Research Foundation of Korea (NRF) grant funded by the Korea government (MSIT) (RS-2023-00219830).

Reference

- Ahamad, F., Griffiths, P. T., Latif, M. T., Juneng, L., and Xiang, C. J.: Ozone Trends from Two Decades of Ground Level Observation in Malaysia, *Atmosphere*, 11, 10.3390/atmos11070755, 2020.
- Ashfold, M. J., Latif, M. T., Mokhtar, A. M., Samah, A. A., Mead, M. I., and Harris, N.: The Relationship between Ozone and Temperature in Greater Kuala Lumpur, Malaysia. *Aerosol Air Qual. Res.*, 24, 240072, 2024.
- Bak, J., Song, E. J., Lee, H. J., Liu, X., Koo, J. H., Kim, J., Jeon, W., Kim, J. H., and Kim, C. H.: Temporal variability of tropospheric ozone and ozone profiles in the Korean Peninsula during the

658 East Asian summer monsoon: insights from multiple measurements and reanalysis datasets, *Atmos.*
659 *Chem. Phys.*, 22, 14177-14187, 10.5194/acp-22-14177-2022, 2022.

660 Cao, T. H., Wang, H. C., Li, L., Lu, X., Liu, Y. M., and Fan, S. J.: Fast spreading of surface ozone in
661 both temporal and spatial scale in Pearl River Delta, *J. Environ. Sci.*, 137, 540-552,
662 10.1016/j.jes.2023.02.025, 2024.

663 Chang, K. L., Petropavlovskikh, I., Cooper, O. R., Schultz, M. G., and Wang, T.: Regional trend
664 analysis of surface ozone observations from monitoring networks in eastern North America,
665 Europe and East Asia, *Elementa*, 5, 10.1525/elementa.243, 2017.

666 Cheesman, A. W., Brown, F., Artaxo, P., Farha, M. N., Folberth, G. A., Hayes, F. J., Heinrich, V. H. A.,
667 Hill, T. C., Mercado, L. M., Oliver, R. J., O' Sullivan, M., Uddling, J., Cernusak, L. A., and Sitch,
668 S.: Reduced productivity and carbon drawdown of tropical forests from ground-level ozone
669 exposure, *Nat. Geosci.* 17, 10.1038/s41561-024-01530-1, 2024.

670 Chen, Z. X., Liu, J. N., Qie, X. S., Cheng, X. G., Yang, M. M., Shu, L., and Zang, Z.: Stratospheric
671 influence on surface ozone pollution in China, *Nat. Commun.*, 15, 10.1038/s41467-024-48406-x,
672 2024.

673 Chen, Z. X., Liu, J. N., Qie, X. S., Cheng, X. G., Shen, Y. K., Yang, M. M., Jiang, R. B., and Liu, X.
674 K.: Transport of substantial stratospheric ozone to the surface by a dying typhoon and shallow
675 convection, *Atmos. Chem. Phys.*, 22, 8221-8240, 10.5194/acp-22-8221-2022, 2022.

676 Colombi, N. K., Jacob, D. J., Yang, L. H., Zhai, S., Shah, V., Grange, S. K., Yantosca, R. M., Kim, S.,
677 and Liao, H.: Why is ozone in South Korea and the Seoul metropolitan area so high and increasing?,
678 *Atmos. Chem. Phys.*, 23, 4031-4044, 10.5194/acp-23-4031-2023, 2023.

679 DeLang, M.N., Becker, J.S., Chang, K.L., Serre, M.L., Cooper, O.R., Schultz, M.G., Schröder, S., Lu,
680 X., Zhang, L., Deushi, M. and Josse, B.: Mapping yearly fine resolution global surface ozone
681 through the Bayesian maximum entropy data fusion of observations and model output for 1990–
682 2017. *Environ. Sci. Tech.*, 55(8), 4389-4398, 2021.

683 Feng, Z. Z., Xu, Y. S., Kobayashi, K., Dai, L. L., Zhang, T. Y., Agathokleous, E., Calatayud, V., Paoletti,
684 E., Mukherjee, A., Agrawal, M., Park, R. J., Oak, Y. J., and Yue, X.: Ozone pollution threatens the
685 production of major staple crops in East Asia, *Nat. Food*, 3, 47-+, 10.1038/s43016-021-00422-6,
686 2022.

687 Gopikrishnan, G. S. and Kuttippurath, J.: Global tropical and extra-tropical tropospheric ozone trends
688 and radiative forcing deduced from satellite and ozonesonde measurements for the period 2005–
689 2020. *Environ. Pollut.*, 361, 124869, 10.1016/j.envpol.2024.124869, 2024.

690 Gu, Y. X., Li, K., Xu, J. M., Liao, H., and Zhou, G. Q.: Observed dependence of surface ozone on
691 increasing temperature in Shanghai, China, *Atmos. Environ.*, 221,
692 10.1016/j.atmosenv.2019.117108, 2020.

693 Jiang, Z. J., Li, J., Lu, X., Gong, C., Zhang, L., and Liao, H.: Impact of western Pacific subtropical
694 high on ozone pollution over eastern China, *Atmos. Chem. Phys.*, 21, 2601-2613, 10.5194/acp-21-
695 2601-2021, 2021.

696 Kawano, N., Nagashima, T., and Sugata, S.: Changes in seasonal cycle of surface ozone over Japan
697 during 1980-2015, *Atmos. Environ.*, 279, 10.1016/j.atmosenv.2022.119108, 2022.

698 Kim, S. W., Kim, K. M., Jeong, Y., Seo, S., Park, Y., and Kim, J.: Changes in surface ozone in South
699 Korea on diurnal to decadal timescales ~~for the~~ for the period of 2001-2021, *Atmos. Chem. Phys.*, 23,
700 12867-12886, 10.5194/acp-23-12867-2023, 2023.

701 Lee, H. J., Chang, L. S., Jaffe, D. A., Bak, J., Liu, X., Abad, G. G., Jo, H. Y., Jo, Y. J., Lee, J. B., and
702 Kim, C. H.: Ozone Continues to Increase in East Asia Despite Decreasing ~~NO₂~~ NO₂:

Causes and Abatements, *Remote Sens.*, 13, 10.3390/rs13112177, 2021.

Lee, H. M. and Park, R. J.: Factors determining the seasonal variation of ozone air quality in South Korea: Regional background versus domestic emission contributions, *Environ. Pollut.*, 308, 10.1016/j.envpol.2022.119645, 2022.

Li, F., Zheng, Q. P., Jiang, Y. C., Xun, A. P., Zhang, J. R., Zheng, H., and Wang, H.: Impact analysis of super Typhoon 2114 'Chanthu' on the air quality of coastal cities in southeast China based on multi-source measurements, *Atmosphere*, 14, 10.3390/atmos14020380, 2023a.

Li, K., Jacob, D. J., Liao, H., Shen, L., Zhang, Q., and Bates, K. H.: Anthropogenic drivers of 2013–2017 trends in summer surface ozone in China, *Proc. Nat. Acad. Sci.*, 116, 422–427, 10.1073/pnas.1812168116, 2019.

Li, K., Jacob, D. J., Shen, L., Lu, X., De Smedt, I., and Liao, H.: Increases in surface ozone pollution in China from 2013 to 2019: anthropogenic and meteorological influences, *Atmos. Chem. Phys.*, 20, 11423–11433, 10.5194/acp-20-11423-2020, 2020.

Li, K., Jacob, D. J., Liao, H., Qiu, Y. L., Shen, L., Zhai, S. X., Bates, K. H., Sulprizio, M. P., Song, S. J., Lu, X., Zhang, Q., Zheng, B., Zhang, Y. L., Zhang, J. Q., Lee, H. C., and Kuk, S. K.: Ozone pollution in the North China Plain spreading into the late-winter haze season, *Proc. Nat. Acad. Sci.*, 118, 10.1073/pnas.2015797118, 2021.

Li, M., Kurokawa, J., Zhang, Q., Woo, J. H., Morikawa, T., Chatani, S., Lu, Z., Song, Y., Geng, G., Hu, H., Kim, J., Cooper, O. R., and McDonald, B. C.: MIXv2: a long-term mosaic emission inventory for Asia (2010–2017), *Atmos. Chem. Phys.*, 24, 3925–3952, 10.5194/acp-24-3925-2024, 2024.

Li, S., Yang, Y., Wang, H. L., Li, P. W., Li, K., Ren, L. L., Wang, P. Y., Li, B. J., Mao, Y. H., and Liao, H.: Rapid increase in tropospheric ozone over Southeast Asia attributed to changes in precursor emission source regions and sectors, *Atmos. Environ.*, 304, 10.1016/j.atmosenv.2023.119776, 2023b.

Liao, Z. H., Ling, Z. H., Gao, M., Sun, J. R., Zhao, W., Ma, P. K., Quan, J. N., and Fan, S. J.: Tropospheric Ozone Variability Over Hong Kong Based on Recent 20 years (2000–2019) Ozone-sonde Observation, *J. Geophys. Res. Atmos.*, 126, 10.1029/2020jd033054, 2021.

Lu, X., Zhang, L., Wang, X. L., Gao, M., Li, K., Zhang, Y. Z., Yue, X., and Zhang, Y. H.: Rapid Increases in Warm-Season Surface Ozone and Resulting Health Impact in China Since 2013, *Environ. Sci. Tech. Lett.*, 7, 240–247, 10.1021/acs.estlett.0c00171, 2020.

Lu, X., Hong, J. Y., Zhang, L., Cooper, O. R., Schultz, M. G., Xu, X. B., Wang, T., Gao, M., Zhao, Y. H., and Zhang, Y. H.: Severe Surface Ozone Pollution in China: A Global Perspective, *Environ. Sci. Tech. Lett.*, 5, 487–494, 10.1021/acs.estlett.8b00366, 2018.

Lu, X., Liu, Y., Su, J., Weng, X., Ansari, T., Zhang, Y., He, G., Zhu, Y., Wang, H., Zeng, G., Li, J., He, C., Li, S., Amnuaylojaroen, T., Butler, T., Fan, Q., Fan, S., Forster, G. L., Gao, M., Hu, J., Kanaya, Y., Latif, M. T., Lu, K., Nédélec, P., Nowack, P., Sauvage, B., Xu, X., Zhang, L., Li, K., Koo, J.-H., and Nagashima, T.: Tropospheric ozone trends and attributions over East and Southeast Asia in 1995–2019: An integrated assessment using statistical methods, machine learning models, and multiple chemical transport models, *EGUsphere*, 10.5194/egusphere-2024-3702, 2024.

Lyu, X., Li, K., Guo, H., Morawska, L., Zhou, B. N., Zeren, Y., Jiang, F., Chen, C. H., Goldstein, A. H., Xu, X. B., Wang, T., Lu, X., Zhu, T., Querol, X., Chatani, S., Latif, M. T., Schuch, D., Sinha, V., Kumar, P., Mullins, B., Seguel, R., Shao, M., Xue, L. K., Wang, N., Chen, J. M., Gao, J., Chai, F. H., Simpson, I., Sinha, B., and Blake, D. R.: A synergistic ozone-climate control to address emerging ozone pollution challenges, *One Earth*, 6, 964–977, 10.1016/j.oneear.2023.07.004, 2023.

- Kang, H., H.-G. Kim, J. Kim, T. Lee, J.-H. Koo, S.-S. Park, Y. Choi, W.-J. Lee, S. A. Shin, and J. Park, Atmospheric and Ozone Profiling Data Measured with Ozonesonde from 2021 to 2024, GEO DATA, 6(4), 561-577, <https://doi.org/10.22761/GD.2024.0041>, 2024. (written in Korean)
- Ma, Z., Xu, J., Quan, W., Zhang, Z., Lin, W., and Xu, X.: Significant increase of surface ozone at a rural site, north of eastern China. *Atmos. Chem. Phys.*, 16(6), 3969-3977, 2016.
- Nagashima, T., Sudo, K., Akimoto, H., Kurokawa, J., and Ohara, T.: Long-term change in the source contribution to surface ozone over Japan, *Atmos. Chem. Phys.*, 17, 8231-8246, 10.5194/acp-17-8231-2017, 2017.
- Neu, J. L., Flury, T., Manney, G. L., Santee, M. L., Livesey, N. J., and Worden, J.: Tropospheric ozone variations governed by changes in stratospheric circulation. *Nat. Geosci.*, 7(5), 340-344, 2014.
- Park, S. S., Kim, J., Cho, H. K., Lee, H., Lee, Y., and Miyagawa, K.: Sudden increase in the total ozone density due to secondary ozone peaks and its effect on total ozone trends over Korea, *Atmos. Environ.*, 47, 226-235, 10.1016/j.atmosenv.2011.11.011, 2012.
- Salvador, C. M. G., Alindajao, A. D., Burdeos, K. B., Lavapiez, M. A. M., Yee, J. R., Bautista, A. T., Pabroa, P. C. B., and Capangpangan, R. Y.: Assessment of Impact of Meteorology and Precursor in Long-term Trends of PM and Ozone in a Tropical City, *Aerosol Air Qual. Res.*, 22, 10.4209/aaqr.210269, 2022.
- Sukkhum, S., Lim, A., Ingviya, T., and Saelim, R.: Seasonal Patterns and Trends of Air Pollution in the Upper Northern Thailand from 2004 to 2018, *Aerosol Air Qual. Res.*, 22, 10.4209/aaqr.210318, 2022.
- Sun, L., Xue, L., Wang, T., Gao, J., Ding, A., Cooper, O.R., Lin, M., Xu, P., Wang, Z., Wang, X. and Wen, L.: Significant increase of summertime ozone at Mount Tai in Central Eastern China. *Atmos. Chem. Phys.*, 16(16), 10637-10650, 2016.
- Sun, H. Z., van Daalen, K. R., Morawska, L., Guillas, S., Giorio, C., Di, Q., Kan, H., Loo, E. X.-L., Shek, L. P., Watts, N., Guo, Y., and Archibald, A. T.: An estimate of global cardiovascular mortality burden attributable to ambient ozone exposure reveals urban-rural environmental injustice, *One Earth*, 7, 1803-1819, <https://doi.org/10.1016/j.oneear.2024.08.018>, 2024.
- Vingarzan, R. (2004). A review of surface ozone background levels and trends. *Atmos. Environ.*, 38(21), 3431-3442, 2004.
- Wang, H., Lu, X., Palmer, P. I., Zhang, L., Lu, K., Li, K., Nagashima, T., Koo, J.-H., Tanimoto, H., Wang, H., Gao, M., He, C., Wu, K., Fan, S., and Zhang, Y.: Deciphering decadal urban ozone trends from historical records since 1980, *Natl. Sci. Rev.*, 11, 10.1093/nsr/nwae369, 2024.
- Wang, H. L., Lu, X., Jacob, D. J., Cooper, O. R., Chang, K. L., Li, K., Gao, M., Liu, Y. M., Sheng, B. S., Wu, K., Wu, T. W., Zhang, J., Sauvage, B., Nédélec, P., Blot, R., and Fan, S. J.: Global tropospheric ozone trends, attributions, and radiative impacts in 1995-2017: an integrated analysis using aircraft (IAGOS) observations, ozonesonde, and multi-decadal chemical model simulations, *Atmos. Chem. Phys.*, 22, 13753-13782, 10.5194/acp-22-13753-2022, 2022b.
- Wang, T., Dai, J. N., Lam, K. S., Nan Poon, C., and Brasseur, G. P.: Twenty-Five Years of Lower Tropospheric Ozone Observations in Tropical East Asia: The Influence of Emissions and Weather Patterns, *Geophys. Res. Lett.*, 46, 11463-11470, 10.1029/2019gl084459, 2019.
- Wang, X. L., Fu, T. M., Zhang, L., Lu, X., Liu, X., Amnuaylojaroen, T., Latif, M. T., Ma, Y. P., Zhang, L. J., Feng, X., Zhu, L., Shen, H. Z., and Yang, X.: Rapidly Changing Emissions Drove Substantial Surface and Tropospheric Ozone Increases Over Southeast Asia, *Geophys. Res. Lett.*, 49, 10.1029/2022gl100223, 2022a.
- Xu, X. B., Lin, W. L., Xu, W. Y., Jin, J. L., Wang, Y., Zhang, G., Zhang, X. C., Ma, Z. Q., Dong, Y. Z.,

793 Ma, Q. L., Yu, D. J., Li, Z., Wang, D. D., and Zhao, H. R.: Long-term changes of regional ozone
794 in China: implications for human health and ecosystem impacts, *Elementa*, 8,
795 10.1525/elementa.409, 2020.

796 Xue, L., Ding, A., Cooper, O., Huang, X., Wang, W., Zhou, D., Wu, Z., McClure-Begley, A.,
797 Petropavlovskikh, I., Andreae, M.O. and Fu, C.: ENSO and Southeast Asian biomass burning
798 modulate subtropical trans-Pacific ozone transport. *Natl. Sci. Rev.*, 8(6), nwaa132, 2021.

799 Ye, X. P., Zhang, L., Wang, X. L., Lu, X., Jiang, Z. J., Lu, N., Li, D. Y., and Xu, J. Y.: Spatial and
800 temporal variations of surface background ozone in China analyzed with the grid-stretching
801 capability of GEOS-Chem High Performance, *Sci. Total Environ.*, 914,
802 10.1016/j.scitotenv.2024.169909, 2024.

803 Yin, Z., Wang, H., Li, Y., Ma, X., and Zhang, X.: Links of climate variability in Arctic sea ice, Eurasian
804 teleconnection pattern and summer surface ozone pollution in North China. *Atmos. Chem. Phys.*,
805 19(6), 3857-3871, 2019.

806 Yuan, S., Stuart, A.M., Laborte, A.G., Rattalino Edreira, J.I., Dobermann, A., Kien, L.V.N., Thúy, L.T.,
807 Paothong, K., Traesang, P., Tint, K.M. and San, S.S.: Southeast Asia must narrow down the yield
808 gap to continue to be a major rice bowl. *Nat. Food*, 3(3), 217-226, 2022.

809 Zanis, P., Akritidis, D., Turnock, S., Naik, V., Szopa, S., Georgoulas, A.K., Bauer, S.E., Deushi, M.,
810 Horowitz, L.W., Keeble, J. and Le Sager, P.: Climate change penalty and benefit on surface ozone:
811 a global perspective based on CMIP6 earth system models. *Environ. Res. Lett.*, 17(2), 024014,
812 2022.

813 Zeng, Y. S., Zhang, J. Q., Li, D., Liao, Z. H., Bian, J. C., Bai, Z. X., Shi, H. R., Xuan, Y. J., Yao, Z. D.,
814 and Chen, H. B.: Vertical distribution of tropospheric ozone and its sources of precursors over
815 Beijing: Results from ~ 20 years of ozonesonde measurements based on clustering analysis, *Atmos.*
816 *Res.*, 284, 10.1016/j.atmosres.2023.106610, 2023.

817 Zhan, C. C. and Xie, M.: Exploring the link between ozone pollution and stratospheric intrusion under
818 the influence of tropical cyclone Ampil, *Sci. Total Environ.*, 828, 10.1016/j.scitotenv.2022.154261,
819 2022.

820 Zhang, J., Li, D., Bian, J., Xuan, Y., Chen, H., Bai, Z., Wan, X., Zheng, X., Xia, X. and Lü, D.: Long-
821 term ozone variability in the vertical structure and integrated column over the North China Plain:
822 results based on ozonesonde and Dobson measurements during 2001–2019. *Environ. Res. Lett.*,
823 16(7), 074053, 2021.

824 Zhang, X. Y., Xu, W. Y., Zhang, G., Lin, W. L., Zhao, H. R., Ren, S. X., Zhou, G. S., Chen, J. M., and
825 Xu, X. B.: First long-term surface ozone variations at an agricultural site in the North China Plain:
826 Evolution under changing meteorology and emissions, *Sci. Total Environ.*, 860,
827 10.1016/j.scitotenv.2022.160520, 2023.

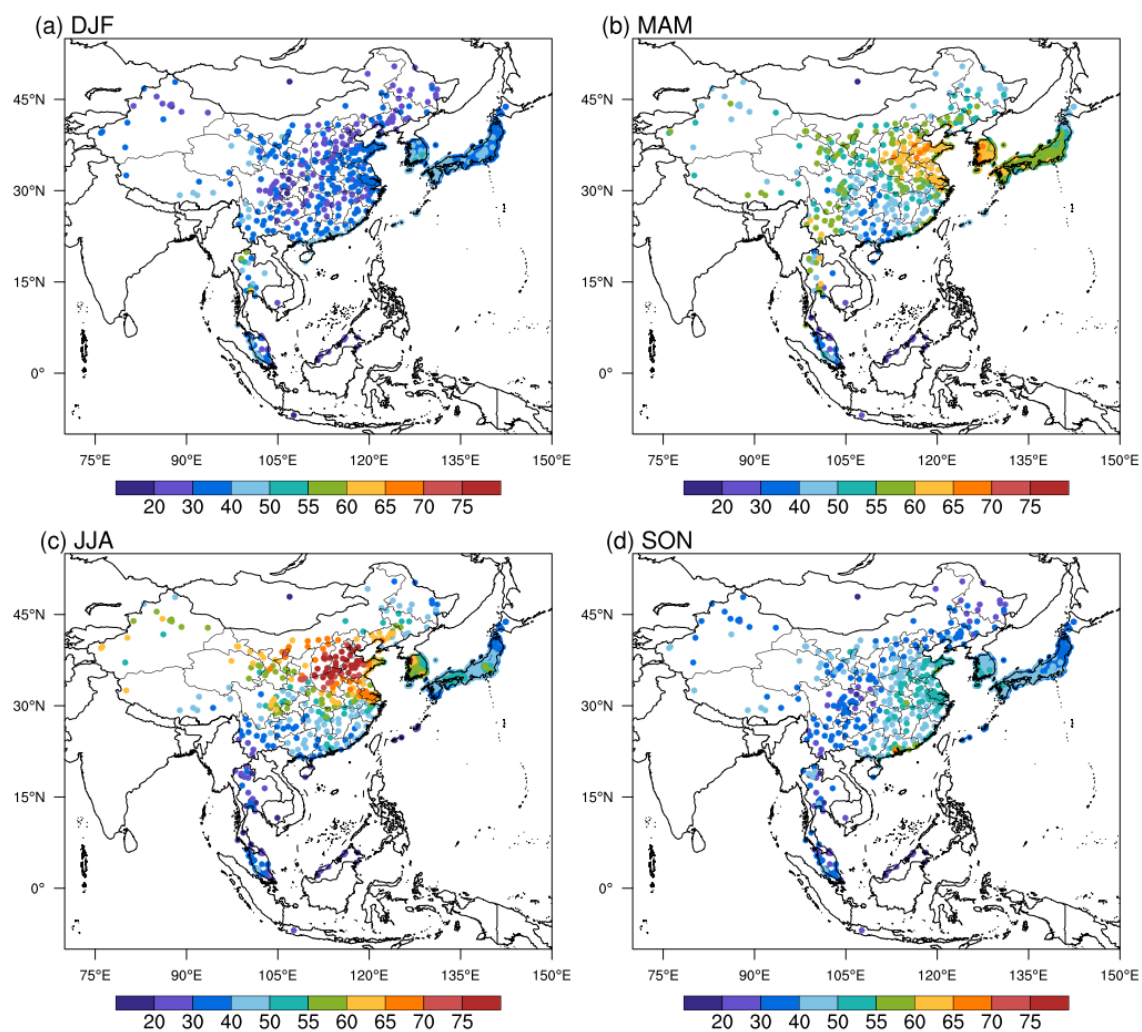
828 Zhang, Y. N., Xiang, Y. R., Chan, L. Y., Chan, C. Y., Sang, X. F., Wang, R., and Fu, H. X.: Procuring
829 the regional urbanization and industrialization effect on ozone pollution in Pearl River Delta of
830 Guangdong, China. *Atmos. Environ.*, 45(28), 4898-4906, 2011.

831 Zhao, Z. J. and Wang, Y. X.: Influence of the West Pacific subtropical high on surface ozone daily
832 variability in summertime over eastern China, *Atmos. Environ.*, 170, 197-204,
833 10.1016/j.atmosenv.2017.09.024, 2017.

834 Zheng, B., Tong, D., Li, M., Liu, F., Hong, C., Geng, G., Li, H., Li, X., Peng, L., Qi, J., Yan, L., Zhang,
835 Y., Zhao, H., Zheng, Y., He, K., and Zhang, Q.: Trends in China's anthropogenic emissions since
836 2010 as the consequence of clean air actions, *Atmos. Chem. Phys.*, 18, 14095–14111,
837 <https://doi.org/10.5194/acp-18-14095-2018>, 2018.

Zhou, H., Yue, X., Dai, H., Geng, G., Yuan, W., Chen, J., Shen, G., Zhang, T., Zhu, J., and Liao, H.: Recovery of ecosystem productivity in China due to the Clean Air Action plan. Nat. Geosci., 17, 1233–1239, 10.1038/s41561-024-01586-z, 2024.

Zhou, Y., Yang, Y., Wang, H., Wang, J., Li, M., Li, H., Wang, P., Zhu, J., Li, K. and Liao, H.: Summer ozone pollution in China affected by the intensity of Asian monsoon systems. Sci. Total Environ., 849, 157785, 2022.



867

868 **Figure 1.** The observed seasonal mean MDA8 ozone (ppb mol^{-1}) in (a) DJF, (b) MAM, (c) JJA,
869 and (d) SON averaged during 2017-2021 over East Asia and Southeast Asia. There are eight countries
870 with surface ozone measurements, including Cambodia (1 site), China (360 sites), Indonesia (1 site),
871 Japan (1187 sites), Malaysia (66 sites), Mongolia (1 site), South Korea (473 sites), and Thailand (25
872 sites).

873

874

875

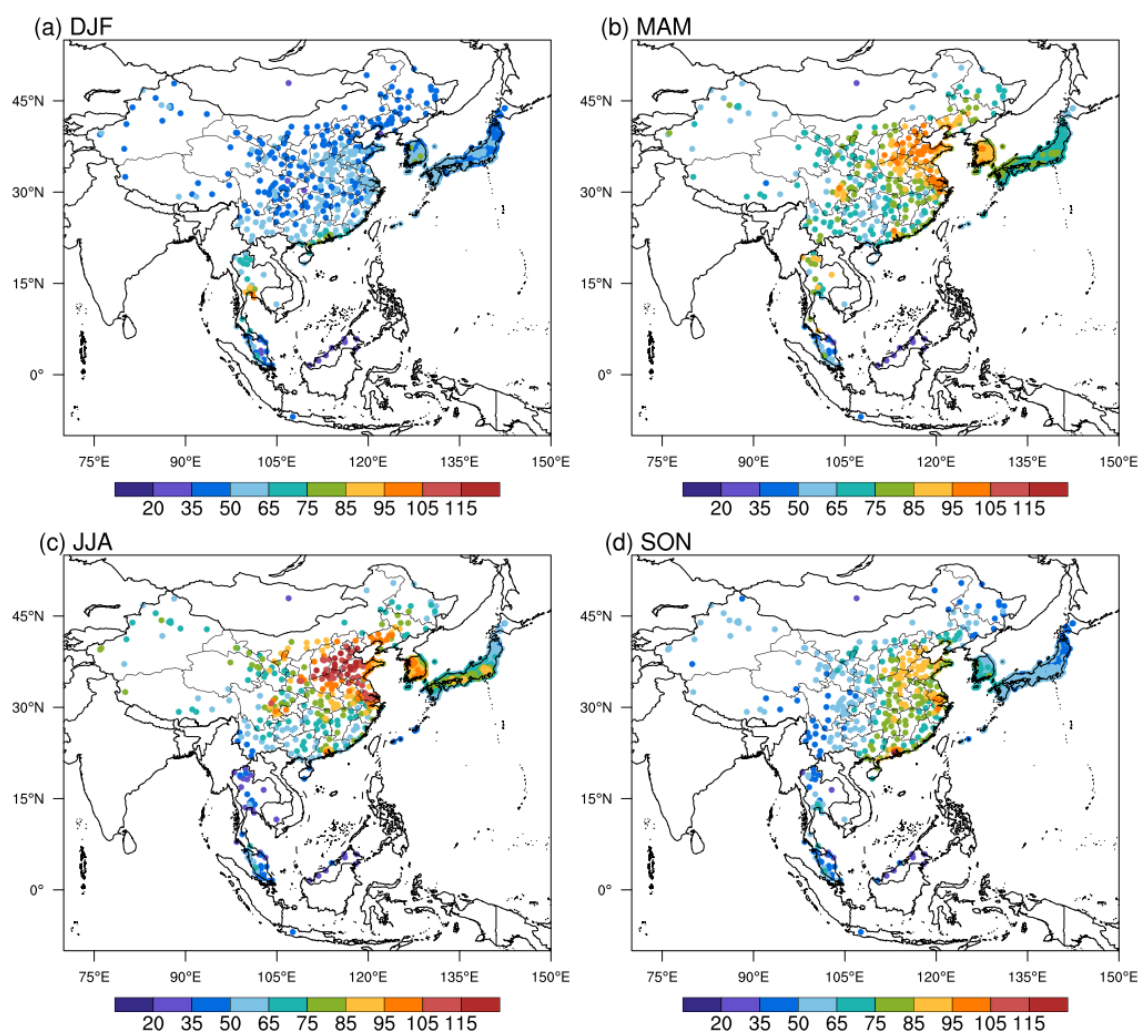


Figure 2. Same as Figure 1 but for the seasonal 95th percentile MDA8 ozone ($\mu\text{mol mol}^{-1}$) averaged over 2017-2021. This metric represents the extreme high ozone values that are related to short-term ozone exposure.

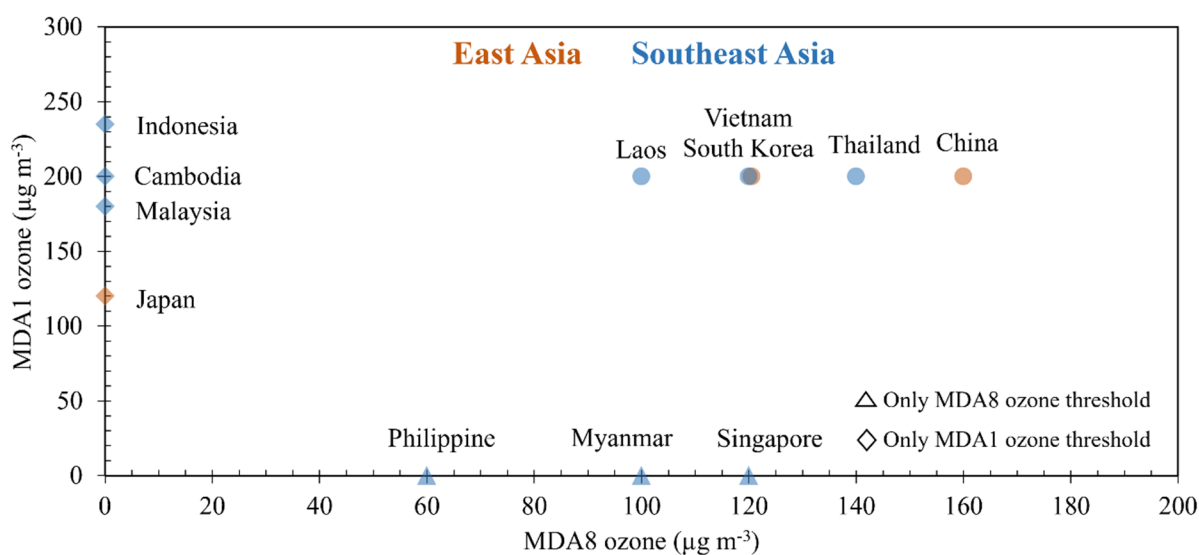


Figure 3. The national ambient ozone air quality standard in East Asia and Southeast Asia. The maximum daily 8 h average (MDA8) and/or maximum daily 1 h average (MDA1) ozone thresholds are routinely adopted but they vary greatly in different countries. The sources for these thresholds are given in Table S1S2. Under standard conditions (1013 hPa, 273 K), $1 \text{ ppb} = 2.14 \text{ µg m}^{-3}$.

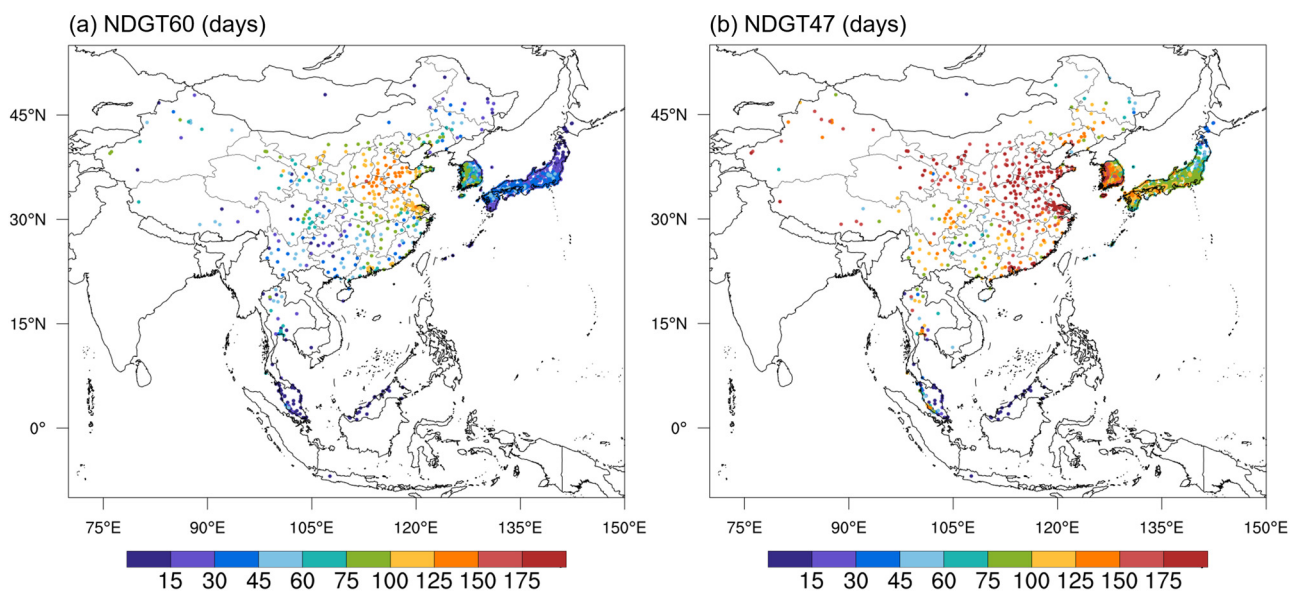


Figure 4. Annual number of days with daily MDA8 ozone greater than 60 ppb (NDGT60) and greater than the WHO standard of $100 \mu\text{g m}^{-3}$ (NDGT47) averaged over 2017-2021. Under standard conditions (1013 hPa, 273 K), $1 \text{ ppb} = 2.14 \mu\text{g m}^{-3}$.

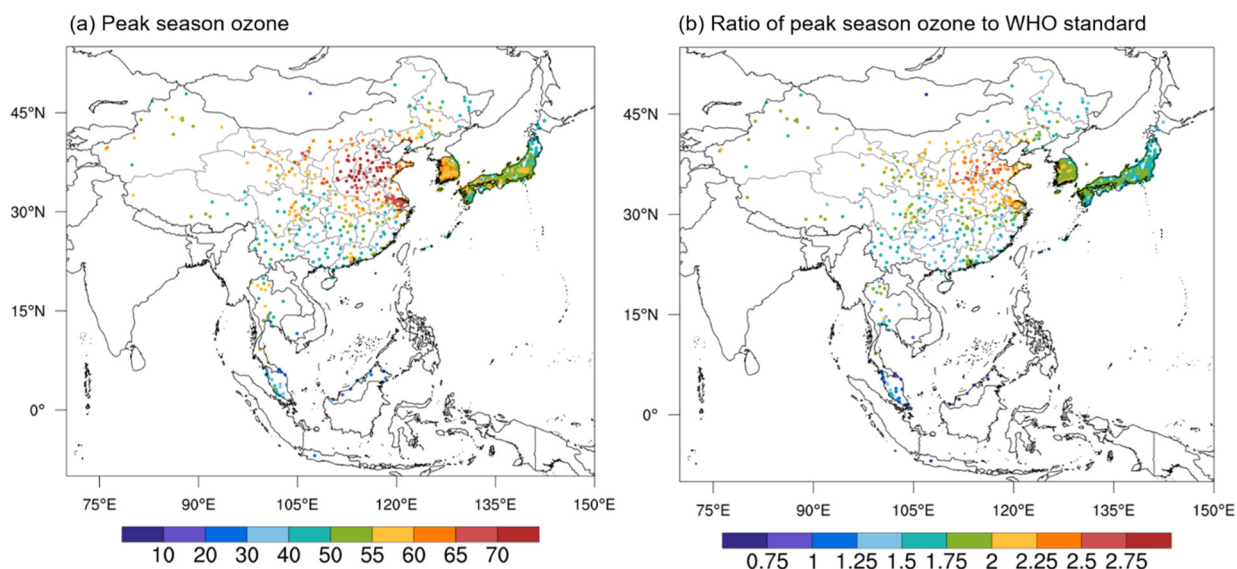
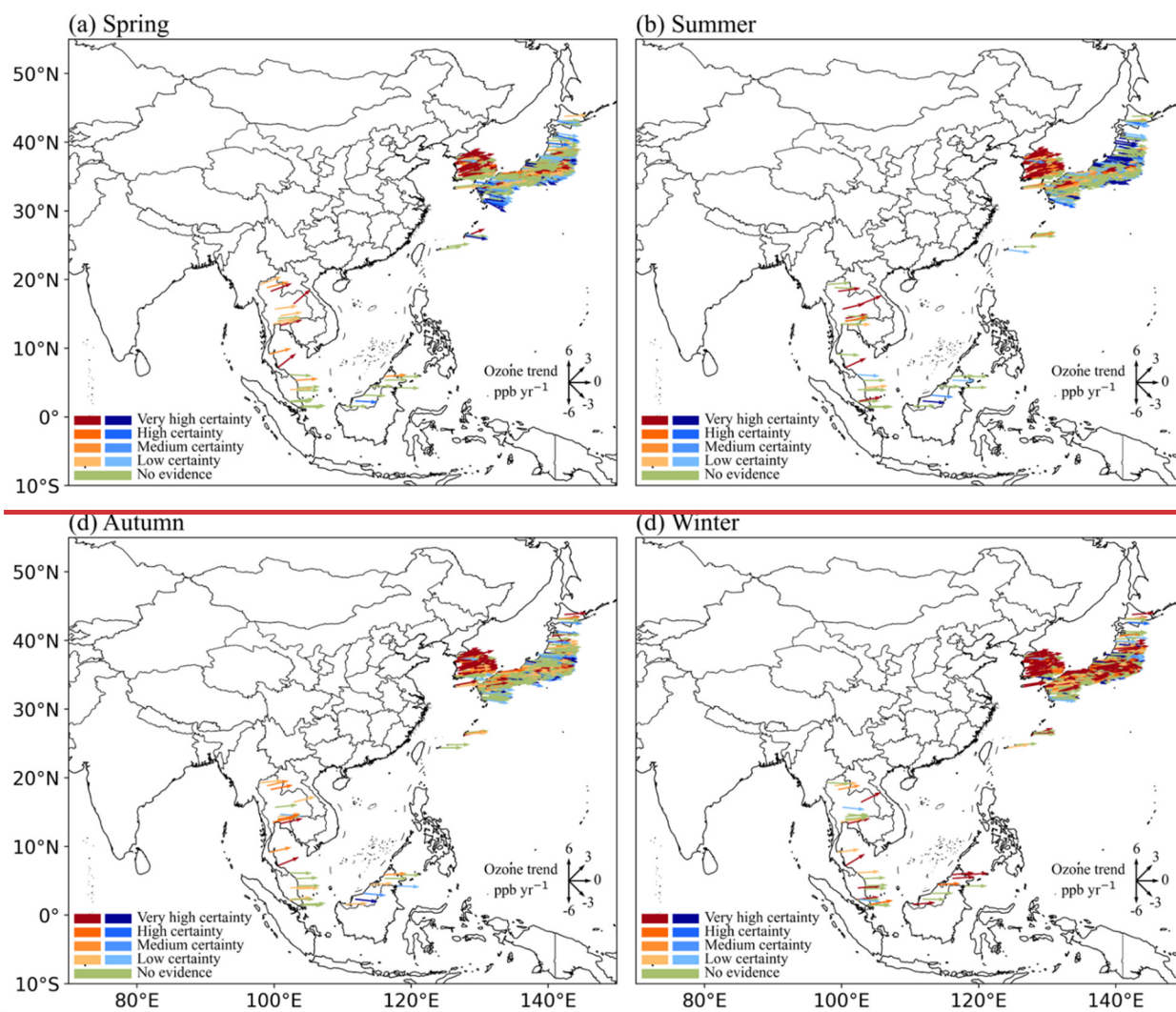


Figure 5. Annual mean peak season ozone ($\mu\text{mol mol}^{-1}$) averaged over 2017-2021 (a) and the ratio of the observed peak season ozone to the WHO standard of $60 \mu\text{g m}^{-3}$ (b). As introduced by the WHO, the concentration of peak season ozone is calculated by using the average monthly MDA8 ozone concentration in the six consecutive months with the highest six-month running-average ozone concentration. This new metric represents the long-term ozone exposure.



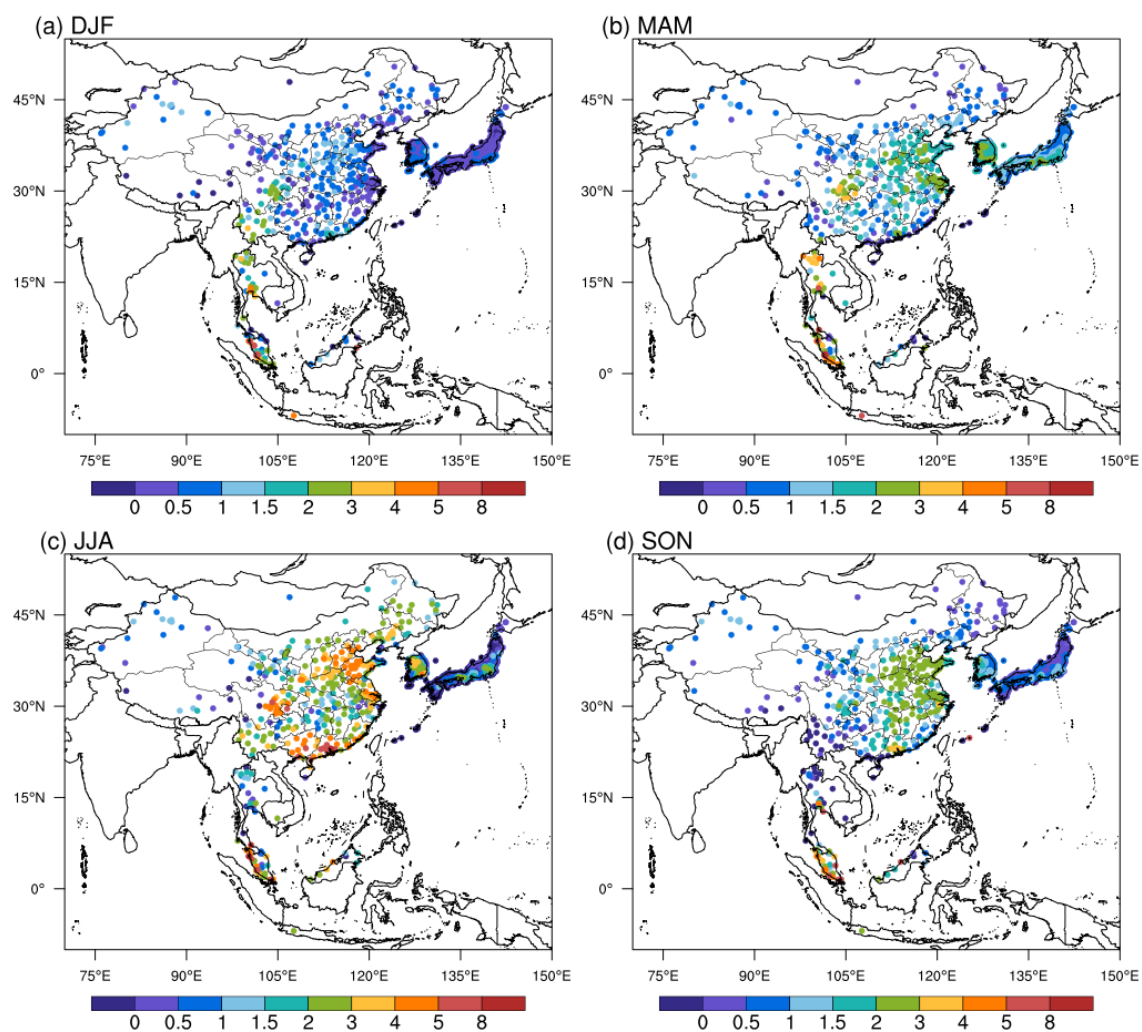


Figure 6. The observed 50th percentile regression slope ($\text{nmol mol}^{-1} \text{ }^{\circ}\text{C}^{-1}$) between daily surface MDA8 ozone and daily maximum 2-m air temperature in (a) DJF, (b) MAM, (c) JJA, and (d) SON averaged over 2017-2021.

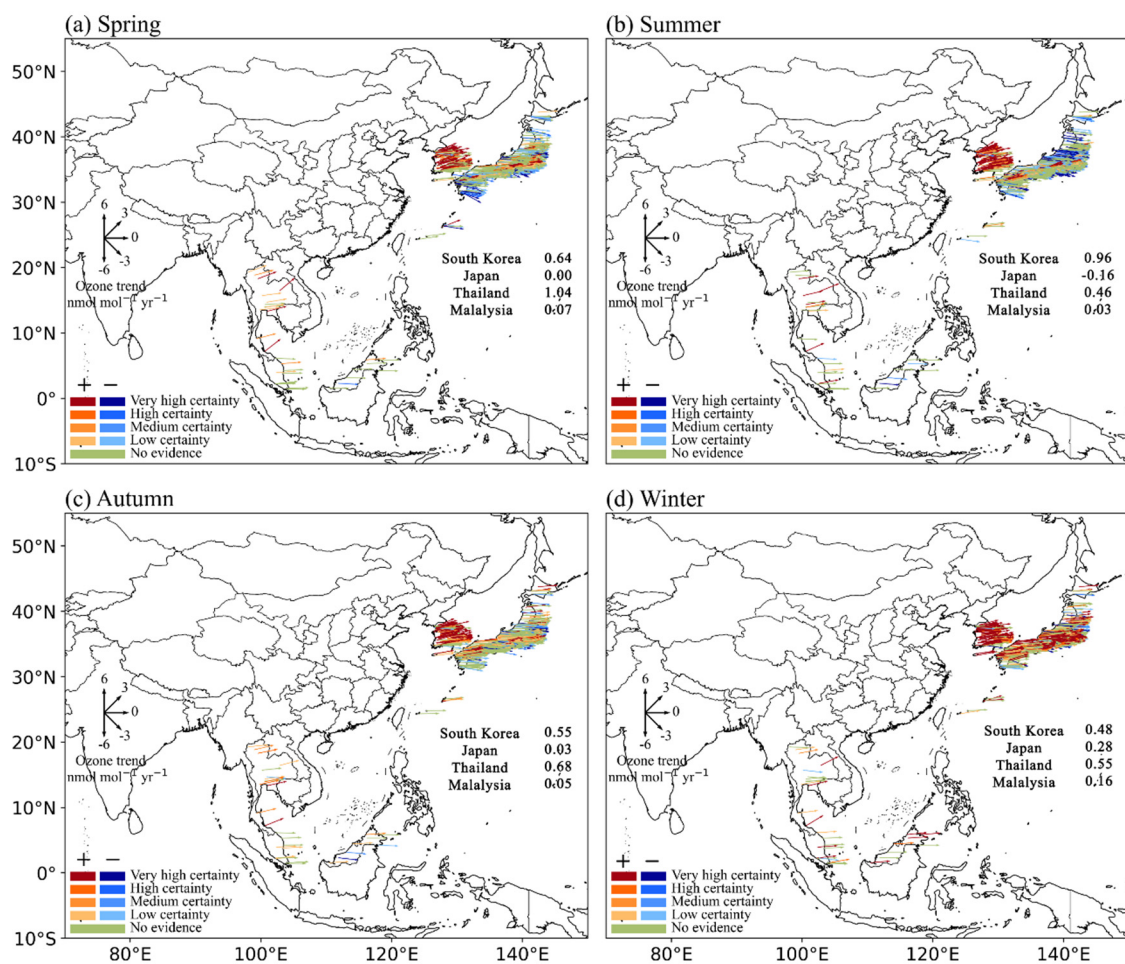


Figure 7. The observed 2005-2021 ozone trends ($\text{nmol mol}^{-1} \text{yr}^{-1}$) during (a) spring, (b) summer, (c) autumn, and (d) winter over East Asia and Southeast Asia. Here it only includes ozone measurements from Malaysia (19 sites), Japan (946 sites), South Korea (226 sites), and Thailand (13 sites). National surface ozone data in China is not available before 2013, therefore not shown in this figure. To follow the trend reliability scale recommended by the TOAR II, here we use “very high certainty” to denote $p \leq 0.01$, “high certainty” to denote $0.05 \geq p > 0.01$, and “medium certainty” to denote $0.10 \geq p > 0.05$; positive trends are in red and negative trends are in blue.

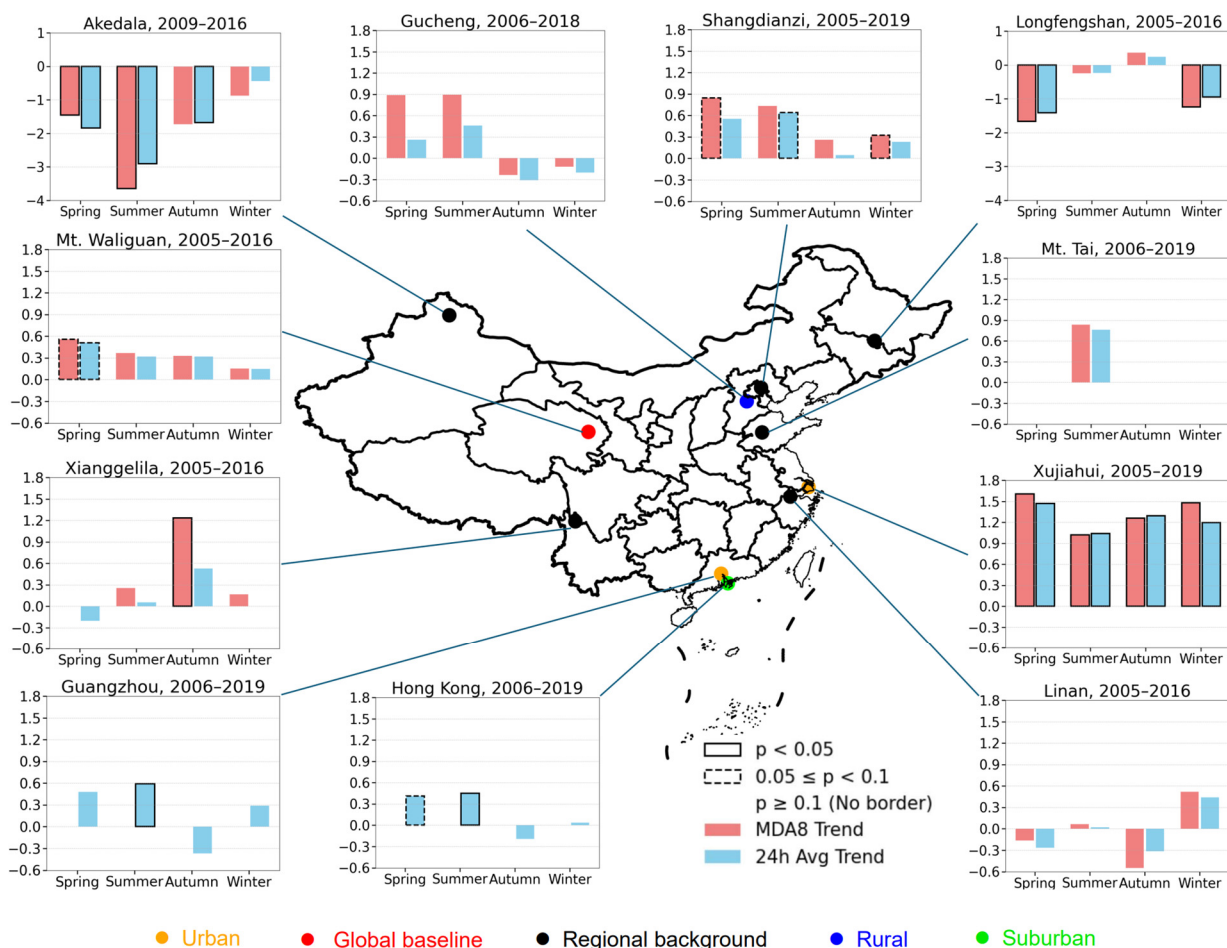
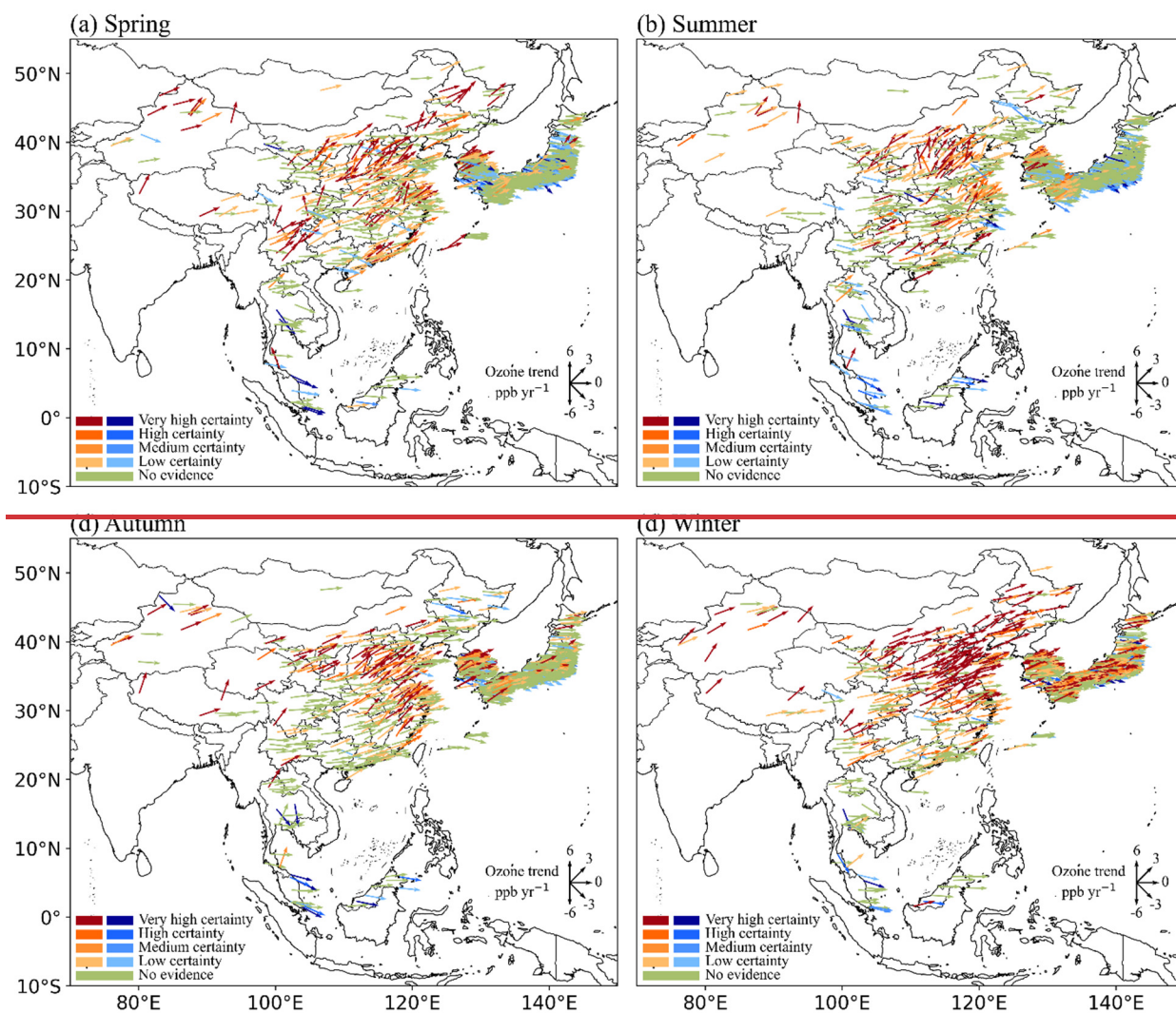


Figure 78. The observed long-term ozone trends ($\text{nmol mol}^{-1} \text{yr}^{-1}$) after 2005 in 11 measurement sites over China. There are 1 global baseline station, 5 regional background stations, 1 rural station, 1 suburban station, and 2 urban stations. Due to data availability, we use the MDA8 ozone and/or 24-hour mean ozone in the calculation of ozone trends. The p-value for estimated ozone trends is also highlighted by rectangles.



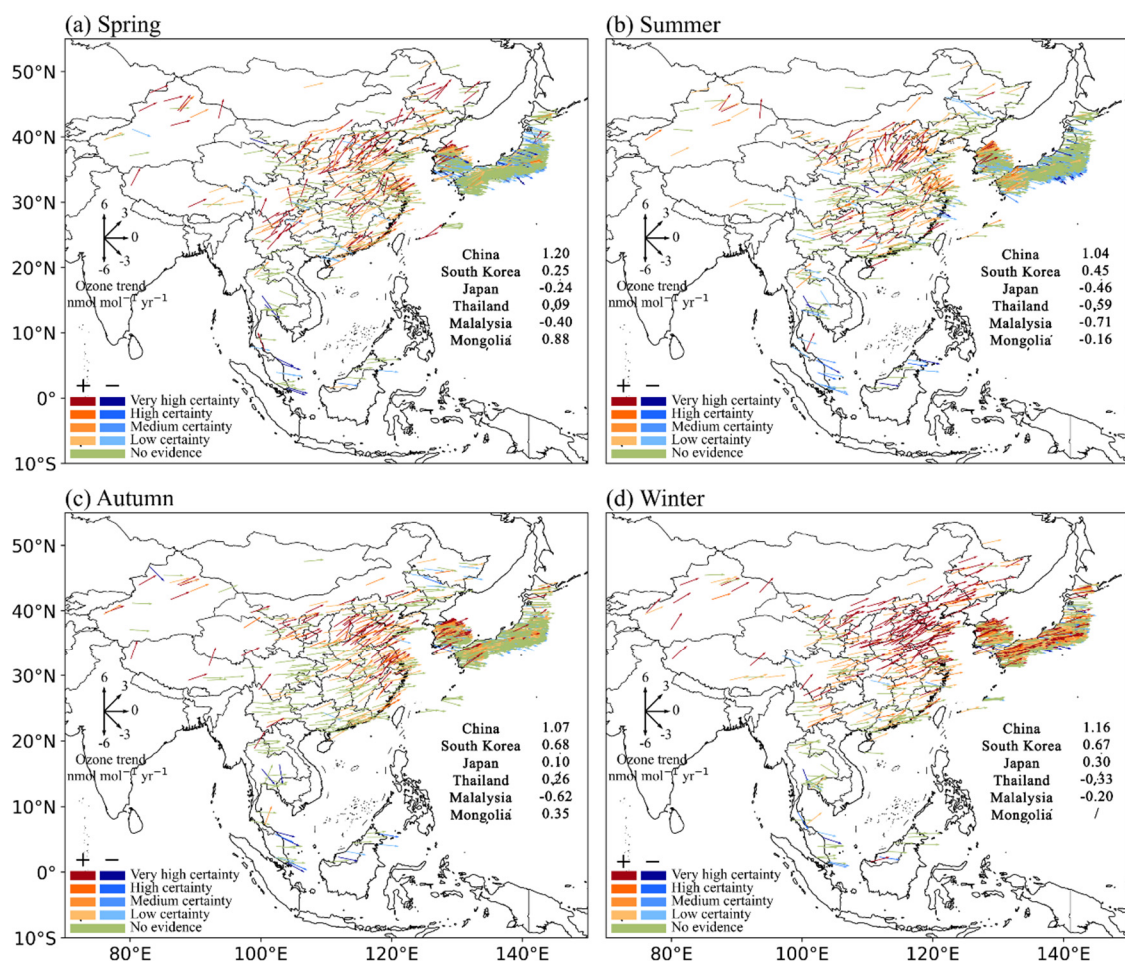


Figure 89. Same with Figure 67 but for the observed 2013-2021 ozone trends ($\text{ppb nmol mol}^{-1} \text{ yr}^{-1}$) over East Asia and Southeast Asia. Here it includes ozone measurements from China (335 sites), Malaysia (19 sites), Mongolia (1 site), Japan (1130 sites), South Korea (270 sites), and Thailand (22 sites). To follow the trend reliability scale recommended by the TOAR II, here we use “very high certainty” to denote $p \leq 0.01$, “high certainty” to denote $0.05 \geq p > 0.01$, and “medium certainty” to denote $0.10 \geq p > 0.05$; positive trends are in red and negative trends are in blue.

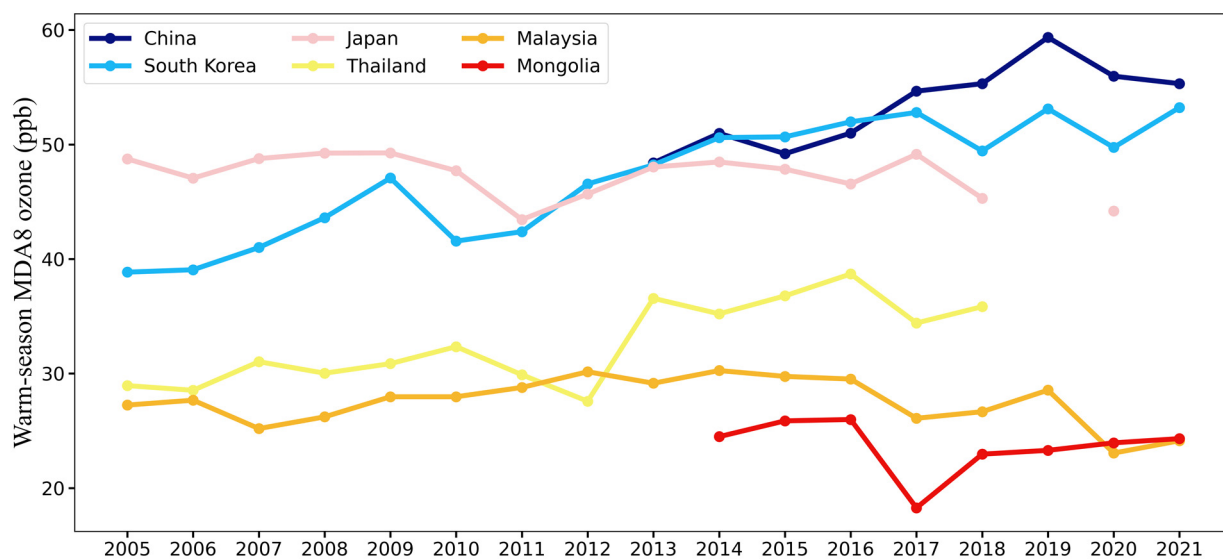


Figure 910. The observed national mean MDA8 ozone (ppb) during warm seasons (April to September) from 2005 to 2021 in East Asia and Southeast Asia.

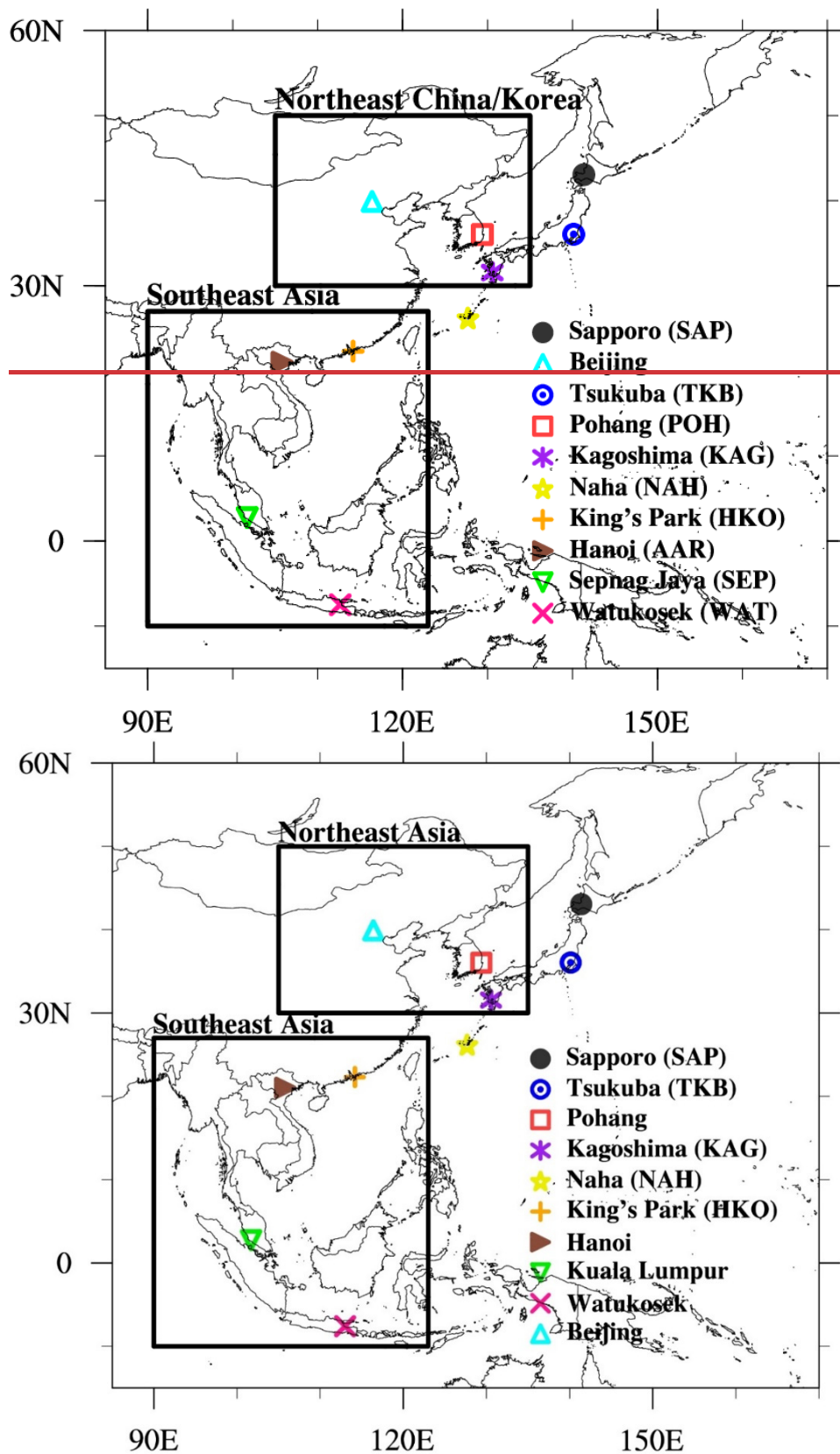


Figure 1011. Map showing the location of ozonesonde sites (symbols) and the coverage of the IAGOS measurements (black box) considered in this study.

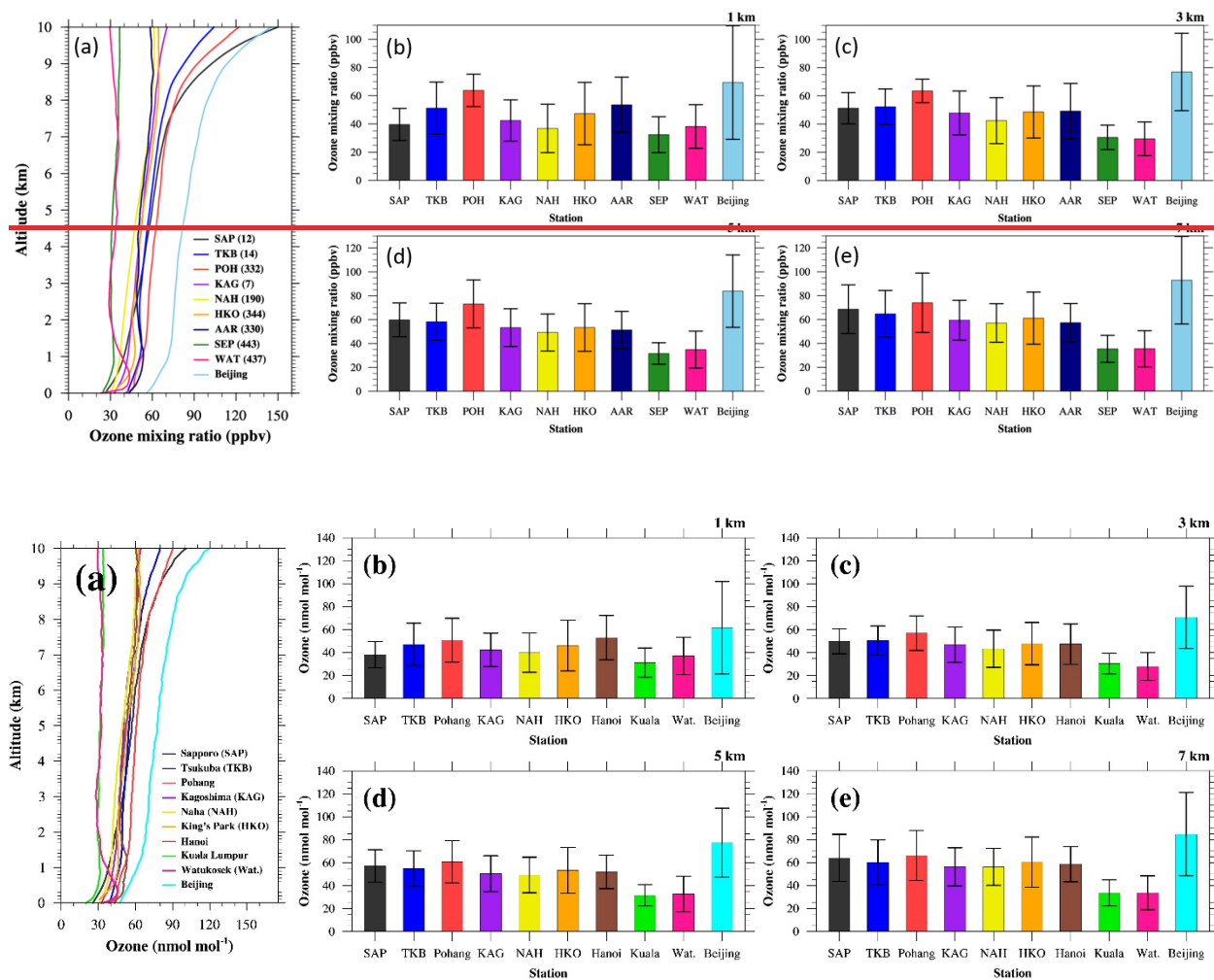


Figure 112. (a) Climatological mean vertical ozone profiles of 10 ozonesonde sites in the troposphere (from 0 to 10 km altitude) are compared. Also, mean ozone mixing ratio values of 10 ozonesonde sites at (b) 1 km, (c) 3 km, (d) 5 km, and (e) 7 km altitude are compared. Error-bar shows the 1-sigma standard deviation range. The number in the parenthesis in panel (a) indicates the number of used data for each site.

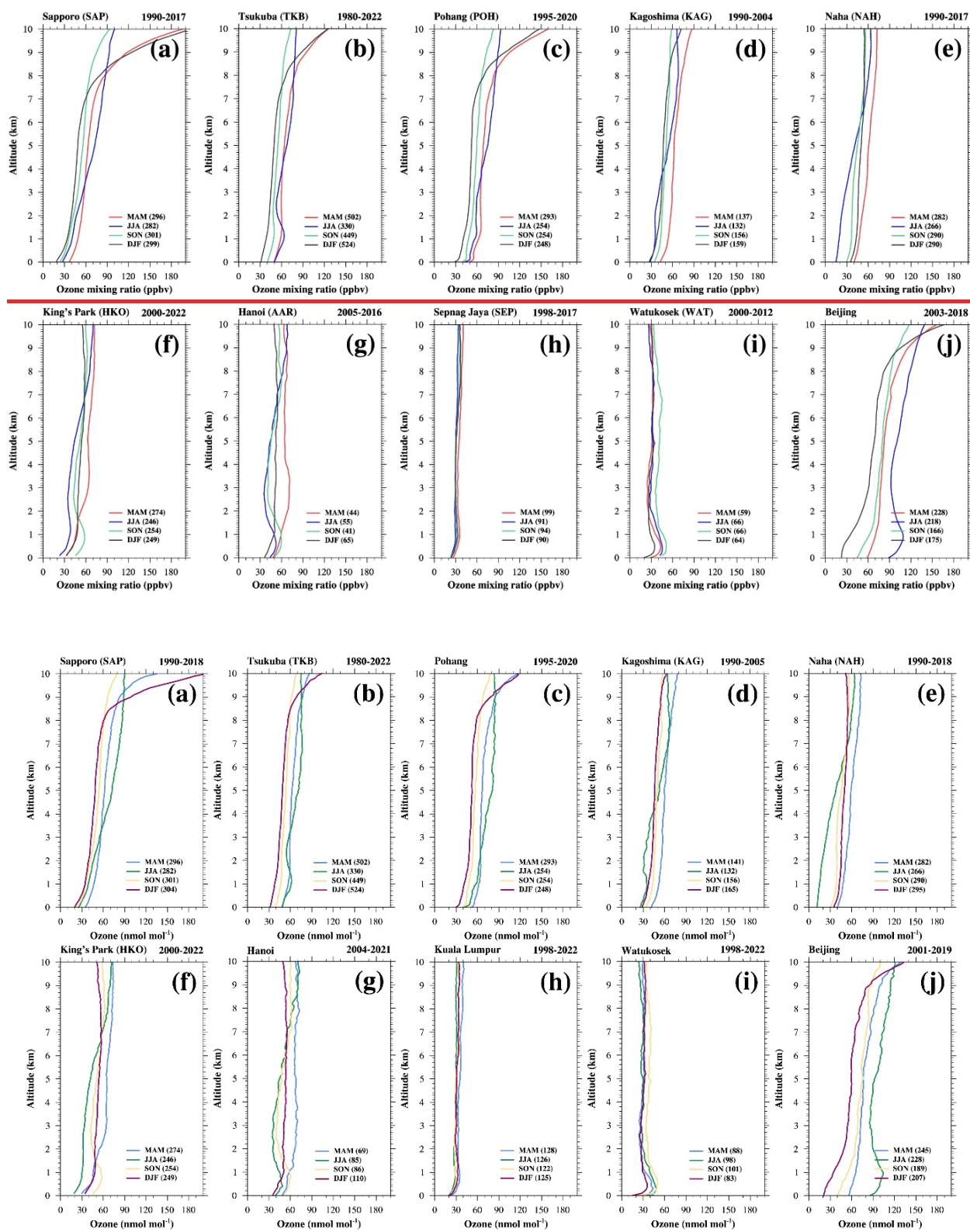
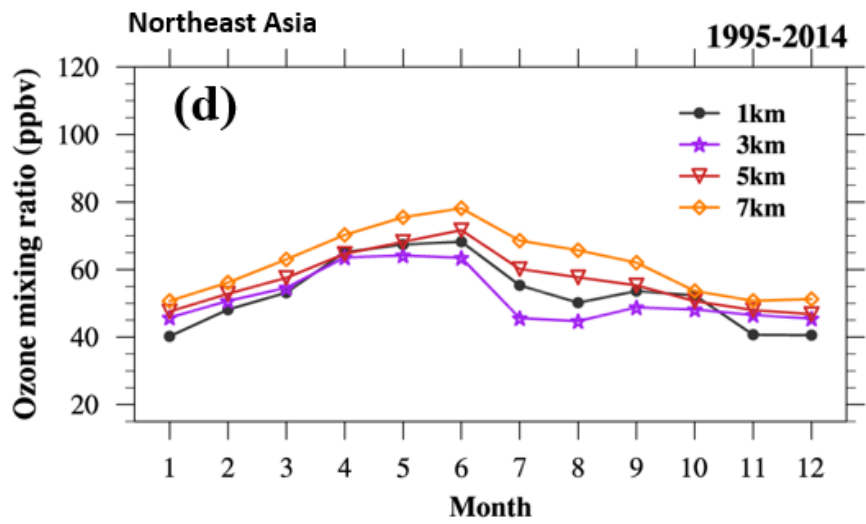
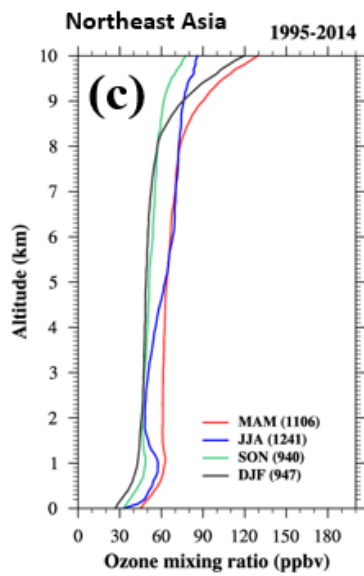
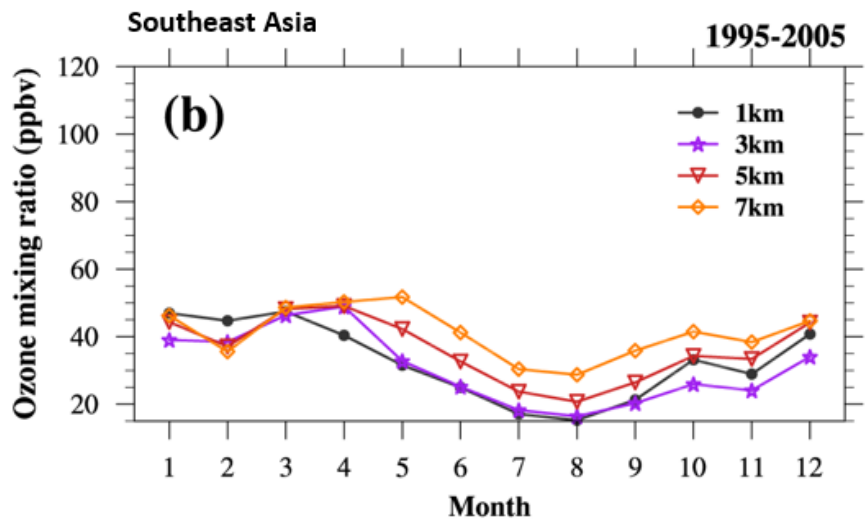
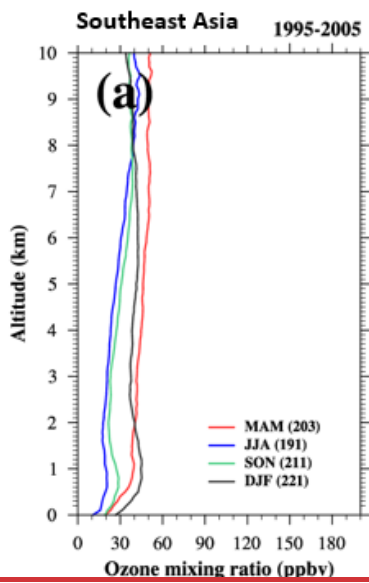


Figure 1213. Seasonal mean vertical ozone profiles at (a) Sapporo (~~SAP~~)₂, (b) Tsukuba (~~TKB~~)₂, (c) Pohang (~~POH~~)₂, (d) Kagoshima (~~KAG~~)₂, (e) Naha (~~NAH~~)₂, (f) King's park (~~HKO~~)₂, (g) Hanoi (~~AAR~~)₂, (h) Sepang Jaya (SEP), Kuala Lumpur, (i) Watukosek, and (j) Beijing site: March-April-May (MAM, ~~redblue~~), June-July-August (JJA, ~~bluegreen~~), September-October-November (SON, ~~greenorange~~), and December-January-February (DJF) ~~-, red~~. The number in the parenthesis of each panel indicates the number of used data for each season.



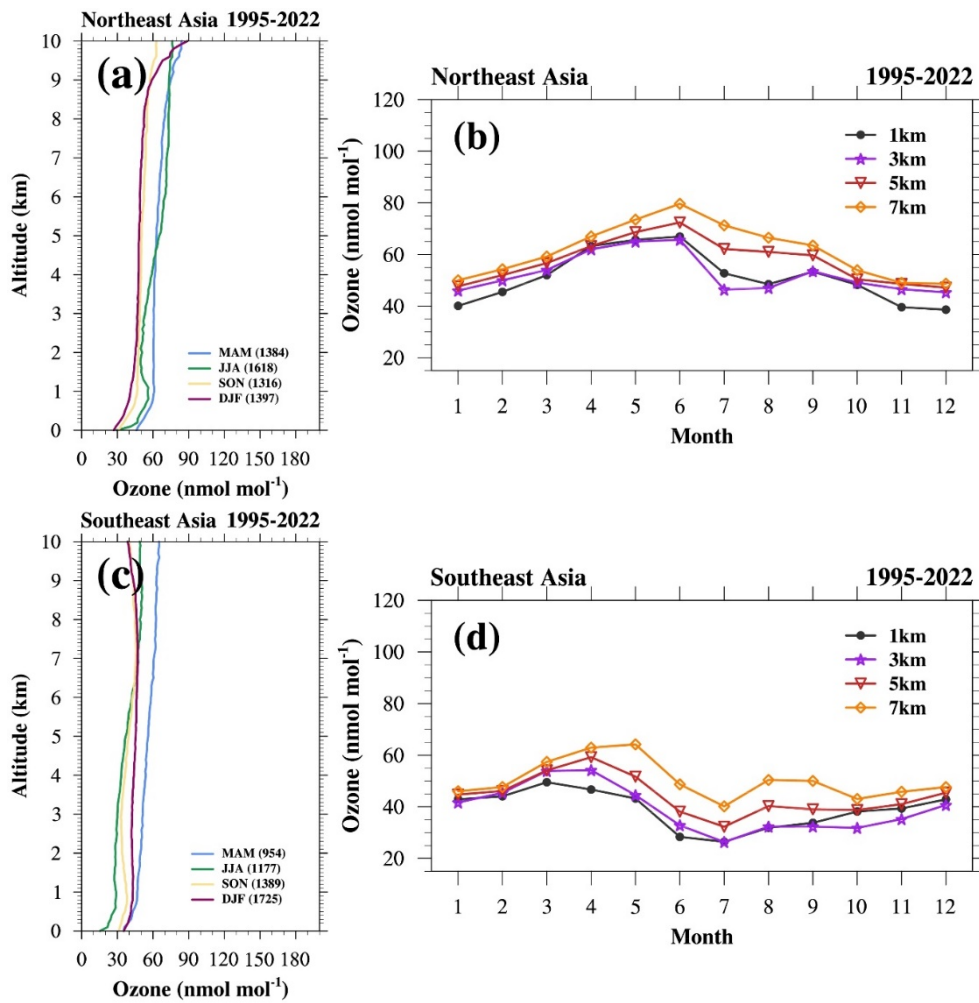


Figure 1314. Analysis of the IAGOS measurements: (a) ~~Seasonal~~seasonal mean vertical ozone profiles in ~~Southeast~~Northeast Asia during March-April-May (MAM, ~~red~~blue), June-July-August (JJA, ~~blue~~green), September-October-November (SON, ~~green~~orange), and December-January-February (DJF, ~~black~~red), (b) monthly mean ozone variation of 1-km (black), 3-km (purple), 5-km (red), and 7-km (orange) altitudes in ~~Southeast~~Asia, (c) ~~seasonal mean vertical ozone profiles in Northeast Asia during MAM (red), JJA (blue), SON (green), and DJF (black), and (d) Monthly mean ozone variation of 1-km (black), 3-km (purple), 5-km (red), and 7-km (orange) altitudes in~~Northeast Asia. (c) same seasonal mean vertical ozone profiles but in Southeast Asia, and (d) same monthly mean ozone variation but in Southeast Asia. The number in the parenthesis in panel (a) and (c) indicates the number of used data for each season.

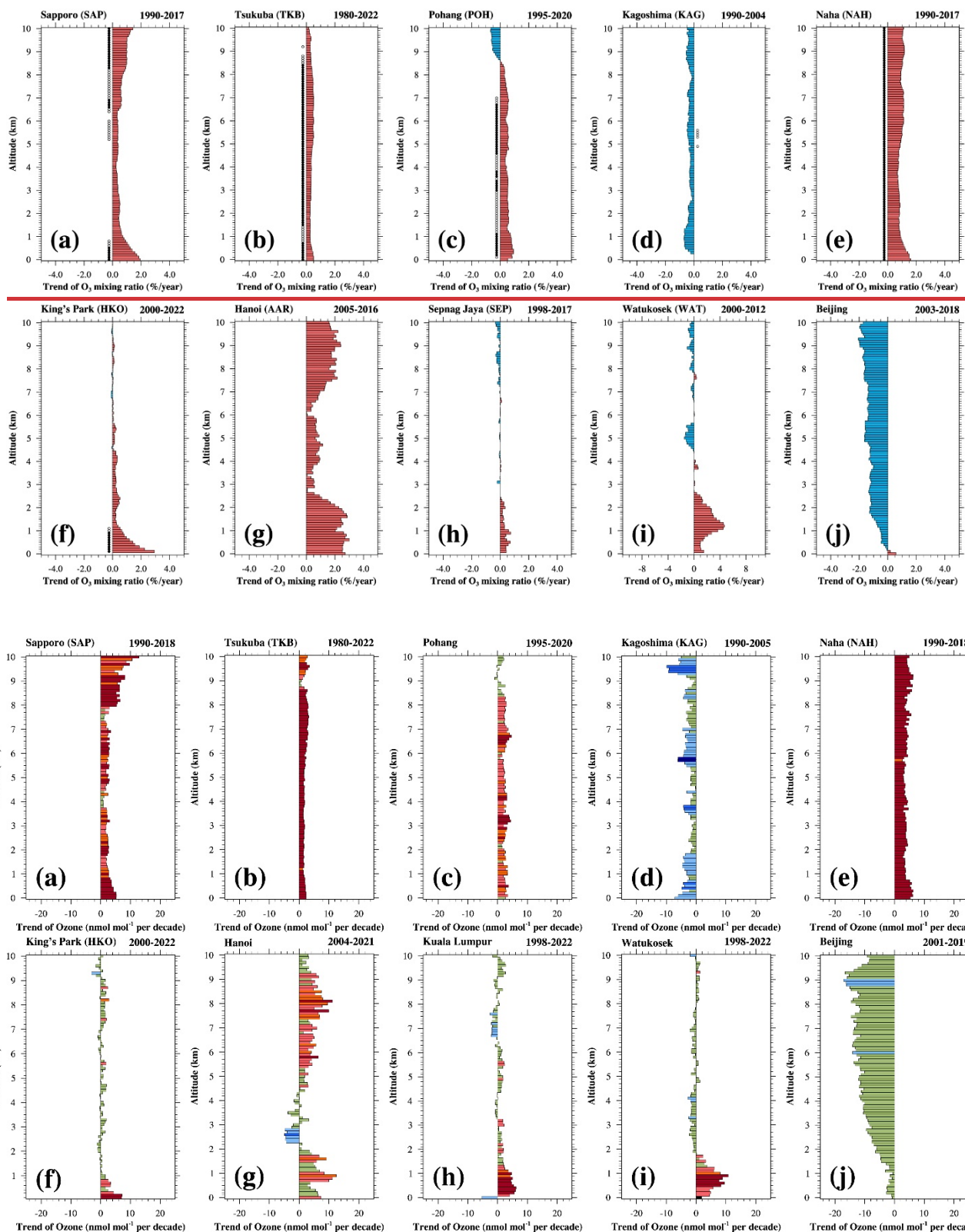


Figure 1415. Long-term trends of annual mean median ozone per 100-m range from 0 to 10 km altitude at (a) Sapporo ~~(SAP)~~, (b) Tsukuba ~~(TKB)~~, (c) Pohang ~~(POH)~~, (d) Kagoshima ~~(KAG)~~, (e) Naha ~~(NAH)~~, (f) King's park ~~(HKO)~~, (g) Hanoi ~~(AAR)~~, (h) Sepang Jaya (SEP), Kuala Lumpur, (i) Watukosek, and (j) Beijing site. Orange Dark red color means increasing, and blue positive trend values with p <= 0.05 (high certainty), orange color means decreasing trend. Black dot indicates that the positive trend is statistically significant having a p-value smaller than 0.01, and white dot does that

~~the~~values with $0.05 < p \leq 0.10$ (medium certainty), light orange color means positive trend is statistically significant having a p -value between 0.01 and 0.05.values with $0.10 < p \leq 0.33$ (low certainty), light olive green color means positive/negative trend values with $p > 0.33$ (no evidence), light blue means negative trend values with $0.10 < p \leq 0.33$ (low certainty), median blue color means negative trend values with $0.05 < p \leq 0.10$ (medium certainty), and dark blue color means negative trend values with $p \leq 0.05$ (high certainty).

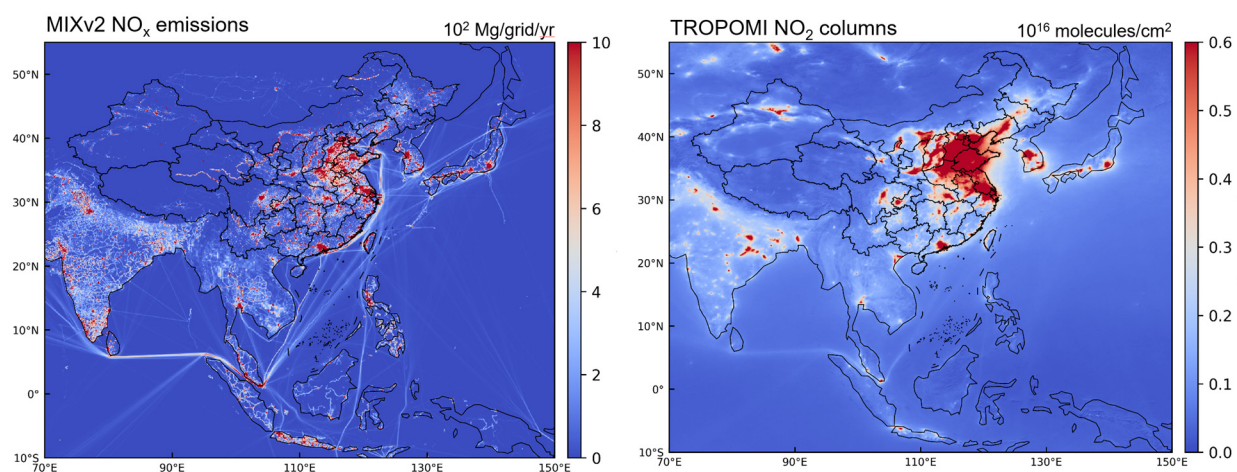


Figure 4516. The spatial distribution of bottom-up NO_x emissions from MIXv2 inventory (left) and the TROPOMI satellite derived NO_2 columns (right). Due to the data availability, emission data for year 2017 and satellite data for year 2019 are used to represent the present-day level (2017-2021), respectively.

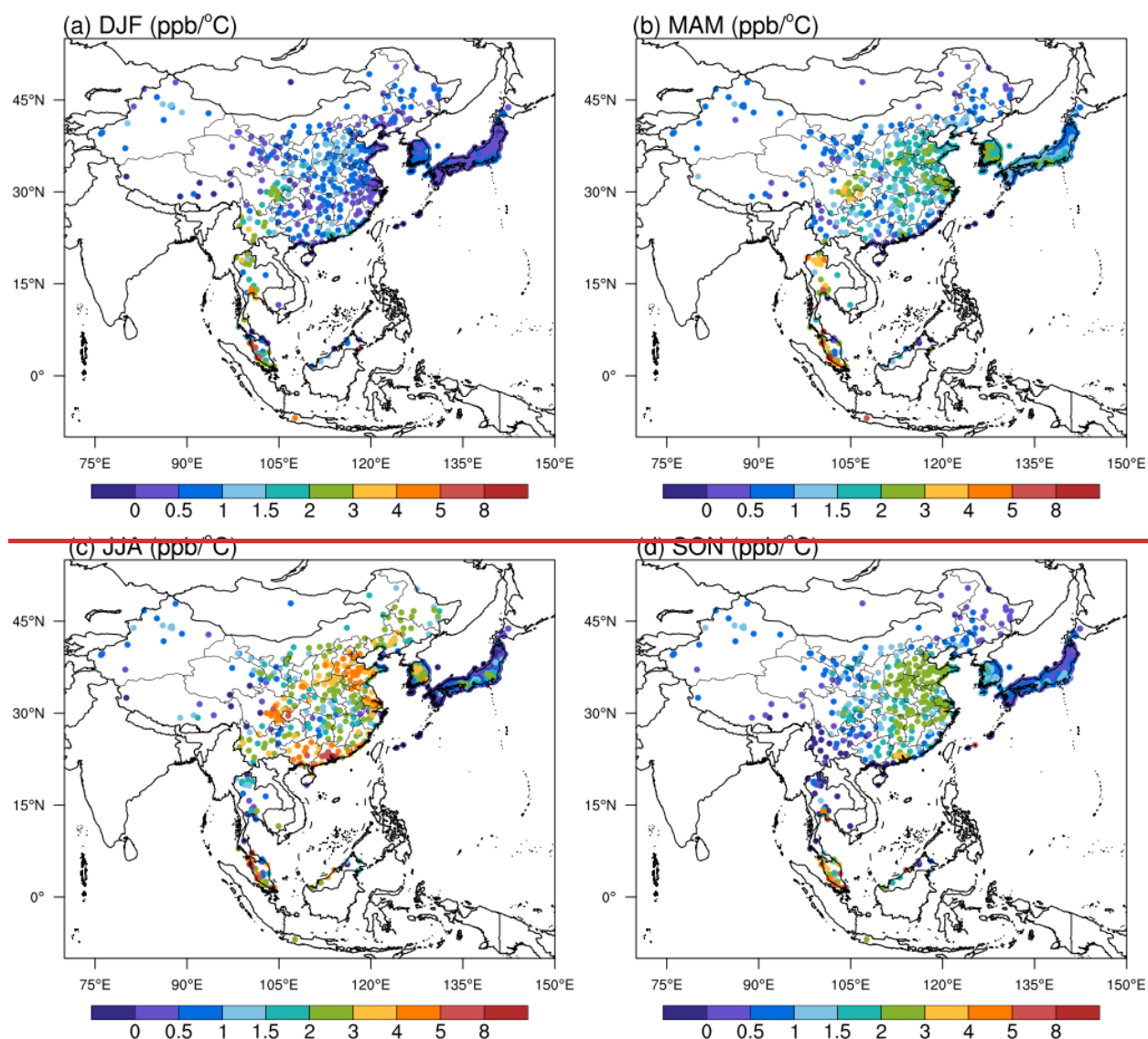


Figure 16. The observed 50th percentile regression slope ($\text{ppb}^{\circ}\text{C}^{-1}$) between daily surface MDA8 ozone and daily maximum 2-m air temperature in (a) DJF, (b) MAM, (c) JJA, and (d) SON averaged over 2017–2021.